Leber's hereditary optic neuropathy (LHON): involvement of mitochondrial permeability transition in the pathogenesis and protective actions of minocycline

Dissertation

zur Erlangung des akademischen Grades

doctor rerum naturalium
(Dr. rer. nat.)

genehmigt durch die Fakultät für Naturwissenschaften
der Otto-von-Guericke-Universität Magdeburg

von

M. Pharm. Mohammad Fahad Haroon

geb. am 13. November 1976 in Aligarh, UP, Indien

Gutachter:

Prof. Gerald Wolf
Prof. Wolfgang Kunz

eingereicht am: 13.12.2007

verteidigt am: 24.06.2008

ACKNOWLEDGEMENTS

First and foremost my thanks and praises to the Almighty Allah who has blessed me with this opportunity and knowledge to proceed further, and a drive to excel in life. Without his guidance and blessings I have no tranquility of mind and no harmony of thought.

I would like to thank wholeheartedly my supervisor and mentor Prof. Gerald Wolf for his willingness to guide me and giving me the chance to work under him. His scientifically directing discussions were the most productive of all. He showed me different ways to approach a research problem and the need to be persistent to accomplish any goal. His constant inspiration kept me motivated.

Thanks to my co-supervisor Dr. Peter Kreutzmann who was actively involved in all the aspects of the project. He was a constant help in my write up and a regular source of motivation. Dr. Elmar Kirches is sincerely thanked for his valued discussions and expert advices. I would like to acknowledge and thank my wife Dr. Ambrin Fatima for her constant help and support throughout.

The admiration I feel towards my heart warming colleagues, Anne Gieseler, Julia Noak, Kathleen Kupsch, and Dr. Gabriella Orlando is indescribable. They were a source of unconditional help, enthusiasm, and friendship. Dr. Thomas Horn, a wonderful teacher, is thanked for his initial grooming and for his directional guidance. He taught me how to ask questions and express my ideas.

I am highly thankful to Dr. G. Keilhoff, Dr. K. Langnaese, Prof. Mario Engelmann, and Dr. K. Richter for their support during the entire course of my study. Special thanks are reserved for Heike Baumann for her excellent technical assistance and for being available for the successful completions of my experiments. Also I am thankful to Leona Bück, Regina Dobrowolny, and Andrea Rudloff for their technical assistance.

This acknowledgement is incomplete without the mention of Julia Czerney and Beate Zörner. I am highly thankful for their administrative help whenever I needed it, and their exuberance

that kept the whole institute lively and an energetic place to work. I would also like to thank the whole staff of "Haus 36" for keeping me on my toes and providing all sort of assistance to carry out my work.

TABLE OF CONTENTS

1.   INTRODUCTION

1.1 Neurodegeneration caused by mitochondrial dysfunction

Neurodegenerative diseases are generally considered as a group of disorders that seriously and progressively impair the functions of the nervous system through selective neuronal vulnerability of specific brain regions. Neurodegeneration is a common theme of many severe diseases, such as Alzheimer's disease, Parkinson's disease, Multiple Sclerosis, Amyotrophic Lateral Sclerosis (ALS), head trauma, epilepsy and stroke. These disorders are devastating for the patient and their families. Furthermore, the annual cost of medical care at present exceeds several hundred billion dollars in the United States alone, and current treatments are inadequate. Adding to the urgency of the problem is the fact that the incidence of these neurodegenerative disorders is increasing rapidly as population demographics change (Kondo 1996). An element of mitochondriopathy has been implicated in most of these neurodegenerative disorders, and is one of the leading areas of research (Lin and Beal, 2006). Among the common neurodegenerative diseases, however, are rare and orphaned diseases which are neglected from therapeutic research, and form a group of diseases subjected to slow and crawling progress. Leber's Hereditary Optic Neuropathy (LHON) is a prime example of such a neurodegenerative disease which is linked to mitochondrial DNA point mutation (Harding and Sweeny, 1994).

Mitochondria are cellular organelles encircled by cardiolipin rich inner membrane (IMM) and surrounded by an outer membrane (OMM). Series of enzyme complexes are present in the IMM known collectively to constitute the electron transport chain (ETC), which is the most effective way for the cell to synthesize ATP by phosphorylation of ADP. The ETC consists of five complexes (Figure 1): complex I or NADH:ubiquinone oxidoreductase contains 41 subunits, complex II (succinate dehydrogenase) contains 5 subunits, cytochrome c reductase or complex III is made up of 11 subunits, complex IV (cytochrome c oxidase) consists of 13 subunits, and complex V (ATP synthase) is composed of 14 subunits. Briefly, the complex I accepts electron from the major donor NADH and couples it with the expulsion of protons from the matrix to the inter-mitochondrial membrane space. The electron moves successive to complex III and complex IV to repeat the expulsion

of protons from both complexes. FADH$_2$, which is also a reducing product of the Kreb's cycle donates its electron to complex II, which again successively passes the electron to complex III and IV. The expelled protons create an electrochemical gradient, which is utilized by complex V to couple the energy of travelling H$^+$ ions (towards the mitochondrial matrix) to oxidative phosphorylation, and ATP production. ETC is also the most important location of free radical generation due to the escape of electrons from the chain during oxidative phosphorylation (mostly at complex I and complex III). This is most certainly obvious with mitochondria harboring defective ETC.

Mitochondrion
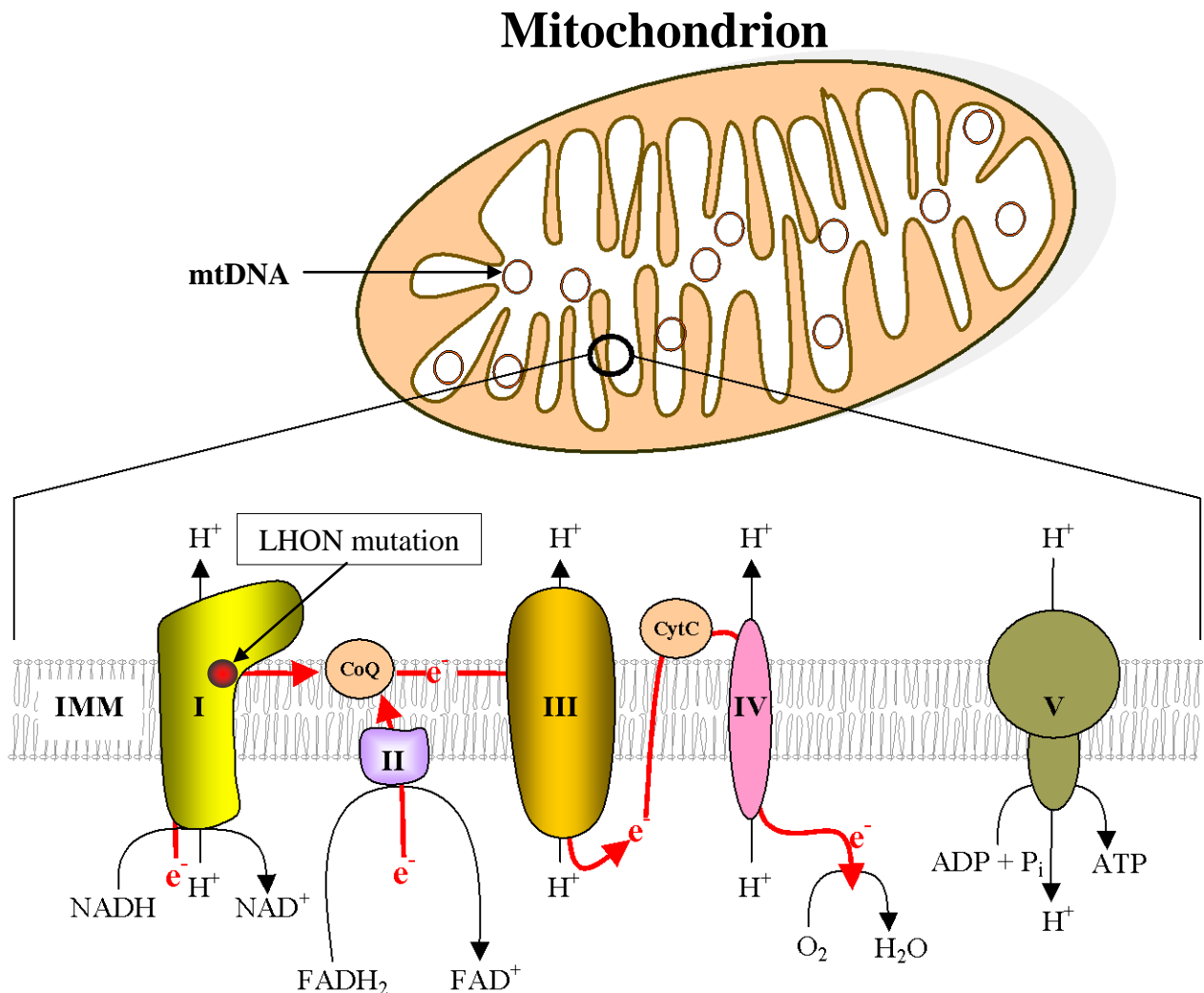
Figure 1: A diagrammatic representation of the electron transport chain (ETC). Complex I-V are labeled with their respective roman numerals, CoQ=coenzyme Q, CytC=cytochrome C, IMM=inner mitochondrial membrane; mtDNA=mitochondrial DNA, H$^+$ represents the proton flow and e$^-$ shows the movement of the electron through the complexes. The resulting LHON mutation is indicated in complex I.

Mitochondria, besides playing the role of energy house of the cell, are unique in the sense that they are the only organelles that contain its own copies of distinct circular DNA within the matrix space. The mitochondrial DNA (mtDNA) is maternally inherited from the ova during fertilization. This circular DNA, which is present at about 100-100000 copies per cell constitutes of 16,569 base pairs with a total of 37 genes, 13 of which are for the structural proteins of the electron transport chain (7 complex I subunits, 1 complex III subunit, 3 complex IV subunits, and 2 complex V subunits). The remaining 24 genes encode for 22 tRNAs and 2 ribosomal RNA molecules, which are necessary for the synthesis of the structural proteins (Weisner et al., 1992).

The rules of mitochondrial genetics differ from those of nuclear DNA (nDNA) in several ways. Firstly, the mtDNA is more prone to mutation as it lies in close proximity of the major ROS producing unit causing oxidative damage, and secondly, it lacks histones that might provide protection. Also a popular belief that the mitochondria do not have adequate repair mechanisms, a view that is no longer valid (Weissman et al., 2007; Bohr and Anson, 1999), has been perceived to contribute to the higher susceptibility of mtDNA damage and to play a role in ageing (Weisner et al., 2006). The circular mtDNA can exist in heteroplasmic forms, i.e. the wild type can coexist with the mutated copies. The phenotypic consequence of the mutation depends on the load of mutated DNA compared to the wild type. If this load exerts a substantial burden then the functional consequence become evident. The heteroplasmic threshold may vary among cells, with the most aerobically active cells being most likely to express the mutation, and therefore to be most affected. Due to the expression of the mutation when the ETC failure or oxidative stress is severe, membrane depolarization occurs. This is most evident in neurons undergoing NMDA toxicity, in which mitochondria accumulate cytosolic calcium and undergo the phenomenon of mitochondrial permeability transition pore (mtPTP) formation preceding apoptosis (Andrabi et al., 2004).

DiMauro enlisted a few mitochondrial diseases as a consequence of mtDNA and nDNA mutation. The listing of diseases due to mtDNA mutation included some of the relatively well known syndromes like LHON, mitochondrial encephalopathy, lactic acidosis, stroke like episodes syndrome (MELAS), and myoclonic epilepsy with ragged-red fibre syndrome (MERRF) along with Person's syndrome and various myopathies due to defective complex I, complex II, and complex III (DiMauro 2004). LHON is among the most

important examples of neurodegenerative diseases caused by mtDNA mutation. Other neurodegenerative diseases like Alzheimer's disease, Parkinson's disease, Huntington's disease and ALS carry an element of dysfunctional mitochondria (Petrozzi et al., 2007), but it is not entirely clear if this is a primary mitochondrial defect. Recent advances in molecular genetics suggest mitochondrial dysfunction in an ever increasing list of degenerative disorders (DiMauro and Davidzon, 2005).

1.2 LOHN disorder: a mitochondriopathy

LHON disorder has been recognized since eighteenth century, when it was mistaken for an infective disease passed on to the child by the carrier mothers. Theodor Leber was the first who described the disorder as a familial neuropathological disease in 1871. Nearly a century later, a novel mode of maternal cytoplasmic inheritance was suggested in the disease (Erickson 1972). Recent advances in research, however, have deciphered the genetic basis of the disease and its link to mtDNA (Brown et al., 1992). A point mutation in the mtDNA affecting the complex I of the respiratory chain leading to high oxidative stress has been claimed responsible for the disorder (Qi et al., 2007a; Battisti et al., 2004; Johns and Colby 2002). LHON is a retinal ganglionic neurodegenerative disorder characterized by an acute or
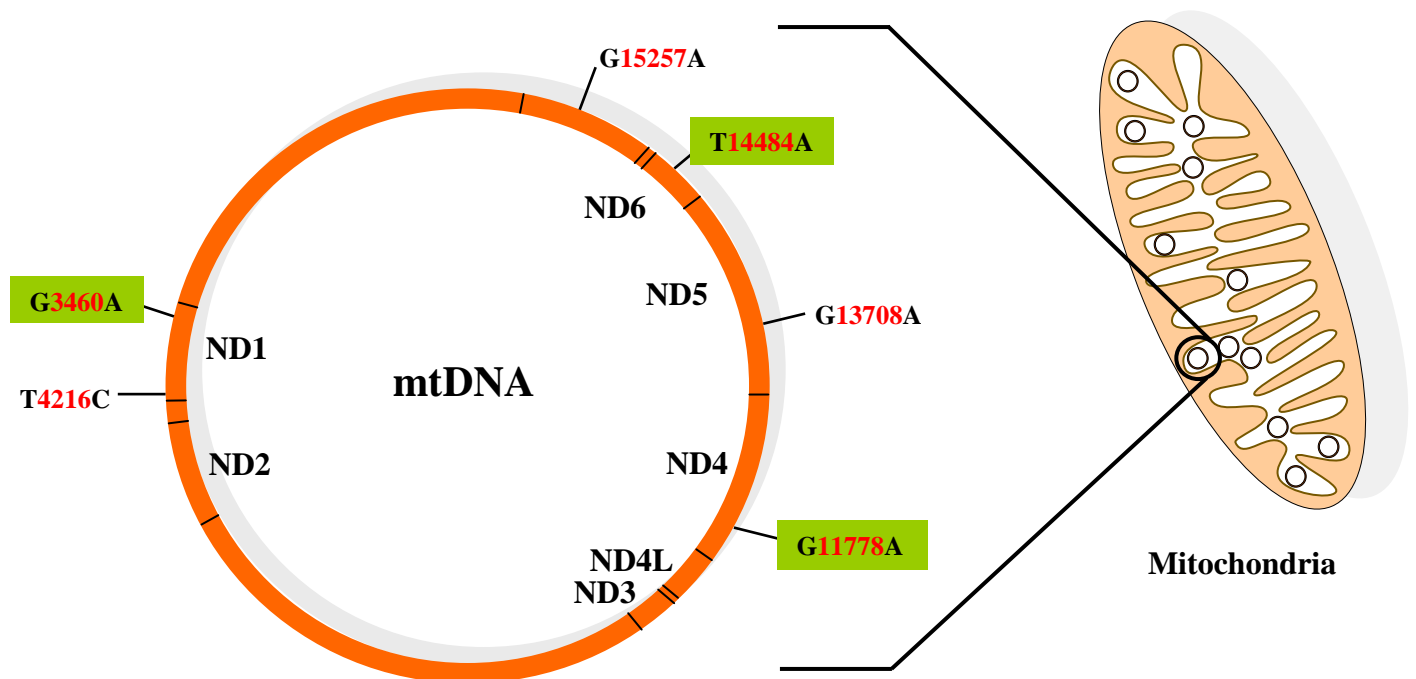

Figure 2: Mitochondrial genome (mtDNA). The seven complex I subunits along with primary LHON mutation (Green background) are presented.

sub-acute, bilateral central vision loss due to degeneration of retinal ganglion cells and the optic nerve. It is occasionally associated with a progressive movement disorder (Novotny et al., 1986; Shoffner et al., 1995). The disorder constitutes to be the commonest cause of blindness in otherwise healthy males. The visual loss is described as fogging or blurring in one eye at first, and eventually in the other with an interval of a few days to months. In most patients the nerve fibre layer around the optic disc is swollen with presence of tortuous retinal arterioles and telangiectasies in the peripapillary small vessels. The age of onset of symptoms tends to be earlier in males (16-30 years) as compared to females (22-63 years), but the clinical symptoms are not markedly different among the sexes (Harding and Sweeney 1994).

The primary cause of LHON disorder is a maternally inherited mtDNA point mutation. Until now, only a handful of definitively proven pathogenic mutations (so called primary LHON mutations) have been established (Figure 2), all of which lead to amino acid exchanges in some subunits of the NADH:ubiquinone-oxidoreductase (complex I) of the respiratory chain. Only three of these mutations located at base pairs 3460, 11778, and 14484 in the mitochondrial genome have been observed most frequently in more than a few families worldwide and contribute to majority of LHON cases (Figure 2). The majority of mutations corresponding to 3460, 11778, and 14484 base pairs of the mitochondrial DNA affect the ND1 (NADH dehydrogenase 1), ND4, and ND6 subunits of the ETC complex I, respectively. There are so far also at least 37 LHON related point mutations of the mtDNA which have been reported (Harding and Sweeney 1994). Wallace et al. previously suggested that the mutation at base pair 11778 was homoplasmic (Wallace et al., 1988), which was then later rectified by studies in the UK suggesting it can be heteroplasmic (Holt et al., 1989).

1.2.1 Epidemiology of LHON

LHON is by far the most frequent disorder of mitochondrial genetic diseases (Carelli et al., 2004b). It occurs with an estimated prevalence of 1 in 25000 people in North East England. About 2 % of registered blinds in Australia suffer from LHON (Man et al., 2003). The prevalence of LHON in Finland is 1:50000, and one in 9000 Finns is a carrier of one of the three LHON primary mutations (Puomila et al., 2007). The 11778 mutation is responsible

for 31-89% of LHON pedigrees in Europe, North America, and Australia and 90% of LHON pedigrees in Japan (Kerrison and Newman, 1997). LHON is also characterized by a marked gender bias, with males more likely to become affected than females and a slight increase in the age of onset in females (Macmillan et al., 1998; Harding et al., 1995; Newman et al,. 1991). Affected females, however, do not have more affected children than unaffected females (Macmillan et al., 1998). There has also been observed a difference in higher incidence of visual recovery among patients with the 14484 mutation compared to the other two most prominent mutations (Johns et al., 1993). Finally, up to 60% of LHON carriers will give a reliable history of other maternal relatives being affected. The remainder most likely represents cases where family history is difficult to trace back, given that *de novo* mutation is rare in LHON.

1.2.2 Pathological pathways in LHON indicate mitochondrial dysfunction

In the 1970s LHON disorder was thought to be an infectious disease transmitted by a virus infecting the child in the uterus of carrier mothers. With the progression of the field of mitochondrial medicine, however, became more evident that the disorder is due to the presence of mtDNA mutation as the primary cause (Swerdlow 2002). Singh and colleagues discovered the presence of the G to A point mutation at the base pair 11778 in the mtDNA in the LHON kindred (Singh et al., 1989). The loss of vision is generally painless, although it can occur with painful eye movements in some patients (Mroczek-Tonska et al., 2003).

Among the mutation harboring population only 50% males and only 10% females actually develop the optic neuropathy. This incomplete penetrance of the mutation suggests additional genetic and environmental factors modulating the phenotypic expression of LHON symptoms (Man et al., 2002). As shown in cybrid (an abbreviation for cytoplasmic hybrid) cell cultures, the amino acid sequence changes of the mitochondrial complex I affect its functioning and lead to a decrease in mitochondrial ATP-synthesis (Baracca et al., 2005). This declined oxidative phosphorylation can lead to decreased ATP levels in cells under conditions blocking non-oxidative ATP generation (Zanna et al., 2005; Zanna et al., 2003; Ghelli et al., 2003). ATP deficiency is thus thought to be one possible explanation of ganglion cell degeneration *in vivo* because the unmyelinated retinal axon sections

theoretically have an extraordinary high energy demand, which is reflected by enhanced cytochrome c oxidase activity (Carelli et al., 2004a). On the other hand, oxidative stress by increased superoxide concentrations may play a role, since complex I is a superoxide generating site of the respiratory chain. Accordingly, reactive oxygen species (ROS) sensitive fluorescent dyes detected higher oxidative stress in mutant cybrid cells (Wong et al., 2002). The decrease in complex I derived ATP production, especially under stressful conditions, and a chronically increased oxidative stress may be the primary responsible factors. ATP deficiency in certain 143B.TK(-) cybrid constructs of LHON mutation have shown to play a vital part in the pathology of the disease which seems to modify the oxidative stress, and the balance between the two modes of cell death (Baracca et al., 2005; Carelli et al., 2004b; Ghelli et al., 2003; Zanna et al., 2003). In addition, calcium overload in the cytoplasm (e.g. following over-excitation) and the mitochondrial matrix may enhance the oxidative stress and thereby increase the probability of opening of mtPTP followed by the release of cytochrome c and apoptosis (Kantrow and Piantadosi, 1997). The declining defensive strength of cellular protection with age and environmentally induced oxidative stress can further provoke the onset of the disease (Kasapoglu and Ozben, 2001, Head et al., 2002). The oxidative stress in the LHON cybrids has also been previously discussed (Floreani et al., 2005). The tissue specific features of retinal ganglionic cells (RGC) may determine the consequence of the disorder. The high energy demanding initial unmyelinated portion of the axons carry a high load of mitochondria and the axonal transport of mitochondria, a process fuelled by mitochondrial ATP, seems to be a crucial step in the functioning of the system. Therefore any bioenergetic defect along with excessive oxidative stress can result in damage to cells, possibly due to triggering of apoptotic pathways (Carelli et al., 2004b).

Another possible cause for the specific damage to the optic nerve was hypothesized by Beretta, showing that the glutamate uptake maximal velocity was significantly reduced in all LHON cybrid cell lines that correlated in a mutation-specific fashion with the degree of mitochondrial production of ROS (Beretta et al., 2004). Their molecular and biochemical analyses showed that excitatory amino acid transporter 1 (EAAT1) was the most active glutamate transporter in their cellular model and the glutamate uptake maximal velocity was significantly reduced in all LHON cybrids compared with control cybrids. This observation is particularly relevant since EAAT1 is the major means of glutamate removal in the inner

retina and prevents retinal ganglion cell death (Rauen et al., 1996). Beretta concluded that the RGC in LHON disorder underwent excitotoxic damage induced by a defective glutamate transport leading to an insufficient withdrawal of retinal glutamate by Mueller cells. Under conditions of mitochondrial dysfunction ROS generation and the probability of mtPTP opening increase, and both are directly related to mitochondrial Ca^{2+} accumulation (Brookes et al., 2004). Evidence of a caspase independent mitochondrial pathway involved in the release of apoptosis inducing factor (AIF) and endonuclease G has also been shown (Zanna et al., 2005). There has been extensive research on the biochemical consequence of the mutations in LHON disorder and elucidation of pathological pathways of the disease like bioenergetic consequence (Carelli et al., 1997; Brown, 1999), biochemical features of the disease (Carelli et al., 1999), and discussion of altered mitochondrial ROS production rendering the retinal ganglion cells vulnerable to apoptotic cell death (Howell, 2003). On the other hand, research in the field of possible pharmacological intervention for the disease is rarely taken up.

1.2.3 Cybrid Cells as model for LHON

The difficulty with studying LHON disease is the dearth of an appropriate model for the disorder. The reason would most obviously be the unavailability of retinal or optic nerve tissue samples or biopsies from patients. By the time the sample or tissue is available the extent of degeneration is already too high. Recently a mouse LHON model, which was developed by the group of John Guy showed for the first time that a transfection of mouse retina with viral vectors, allotopically expressing a mutant human ND4 subunit, did develop elevated ROS production, optical nerve head swelling, apoptosis and progressive loss of retinal ganglion cells (Qi, et al., 2007b). These effects did not occur in mice transfected with human wild type ND4. This is the first true genetic animal model of LHON. The cybrid cell technology also provides us with a unique opportunity to study the disorder as they are relatively easy to produce and can be used for an initial high throughput screening of drugs.

Yeast cells capable of switching from aerobic to anaerobic conditions for their survival needs is an example of naturally depleting mtDNA. Attempts of inducing mtDNA depletion experimentally in cultured cells have resulted in the so called "rho-zero (ρ0) cells"

(Desjardins et al. 1986). Such cells can survive under the right conditions of culture and nutritional support. The cybridization procedure involves depleting of mtDNA from the cells by ethidium bromide treatment, and finally fusing the resulting ρ0 cells with mitochondria rich platelets or enucleated fibroblast (obtained from patients with mtDNA mutation) with the ρ0 cells. With time the donor mtDNA will repopulate the ρ0. Thereafter, removing the nutritional supplements supporting the survival of ρ0 cells would naturally select the properly cybridized cells. The cybrid technology lends itself to study the LHON disorder, as the degenerating optic nerve is generally not accessible until the death of the patient, by which time the severity of the ailment is to its maximum with degeneration to full extent. In addition, the model allows a direct comparison of cell clones with mutant or wild type mtDNA, but containing identical nuclear DNA. The model could also provide a valuable tool to assess and correlate to other diseases of a possibly similar pathology e.g. Parkinson's, Alzheimer's, and Huntington's disease.

1.3 Role of calcium

The role of calcium can not be ignored in the pathology of mitochondrial disorders as mitochondria are the primary calcium buffering organelles. With over-excitation, especially in neurons, cells can undergo a state of increased cytosolic calcium levels, which can act as a signal for apoptosis and cell death by its uptake into the mitochondria. The pathway of calcium in the mitochondria starts primarily through voltage dependent anion-selective channel (VDAC) in the OMM (Gincel et al., 2001; Rapizzi et al., 2002) and then through the uniporter in the IMM (Kirichok et al., 2004) (Figure 3). The molecular nature of the uniporter remains unknown but it is identified as highly selective for calcium ions (Ca^{2+}). The driving force for uptake of Ca^{2+} comes from a fact that the mitochondrial membrane potential is highly negative and can quickly take up cations. This energy independent uptake nevertheless causes depletion of ATP by hydrolysis of ATP to drive H^+ accumulation to regenerate the membrane potential through the reversal of H^+-ATPase (Jacobson and Duchen 2004). The calcium entering the mitochondria is a stimulus for the respiration by acting on the Ca^{2+} sensitive mitochondrial dehydrogenase which increases the production of hydrogen ions to drive the maintenance of the negative membrane potential as well as the production of ATP (Denton and McCormack, 1986). Increased matrix calcium also interacts with cyclophilin D (which is a component of the mtPTP). Also ROS (Starkov et al., 2004) and

free fatty acid (Scorrano et al., 2001) generation are promoted by a rise in mitochondrial Ca^{2+}. These factors further promote the formation of mtPTP. The mtPTP is proteinaceous and composed of three important proteins, namely voltage dependent anionic channel (VDAC) at the OMM, adenosine nucleotide translocase (ANT) at the IMM, and cyclophilin D at the matrix side (Tsujimoto et al., 2006; Crompton, 1999). The mtPTP-opening causes dissipation of the mitochondrial membrane potential with the release of Ca^{2+} and accumulation of solutes in the mitochondrial matrix. Local Ca^{2+} transfer between adjoining domains of the endoplasmic / sarcoplasmic reticulum (ER/SR) and mitochondria allows ER/SR Ca^{2+} release to activate mitochondrial Ca^{2+} uptake and evoke a matrix Ca^{2+} rise. High matrix Ca^{2+} thereby exerts control on several steps of energy metabolism and synchronizes ATP generation with cell functions. However, under conditions of high calcium loads and oxidative stress, calcium signal propagation to the mitochondria may also ignite a cell death program through permeability transition, facilitated by a pore formed in the inner membrane. This occurs
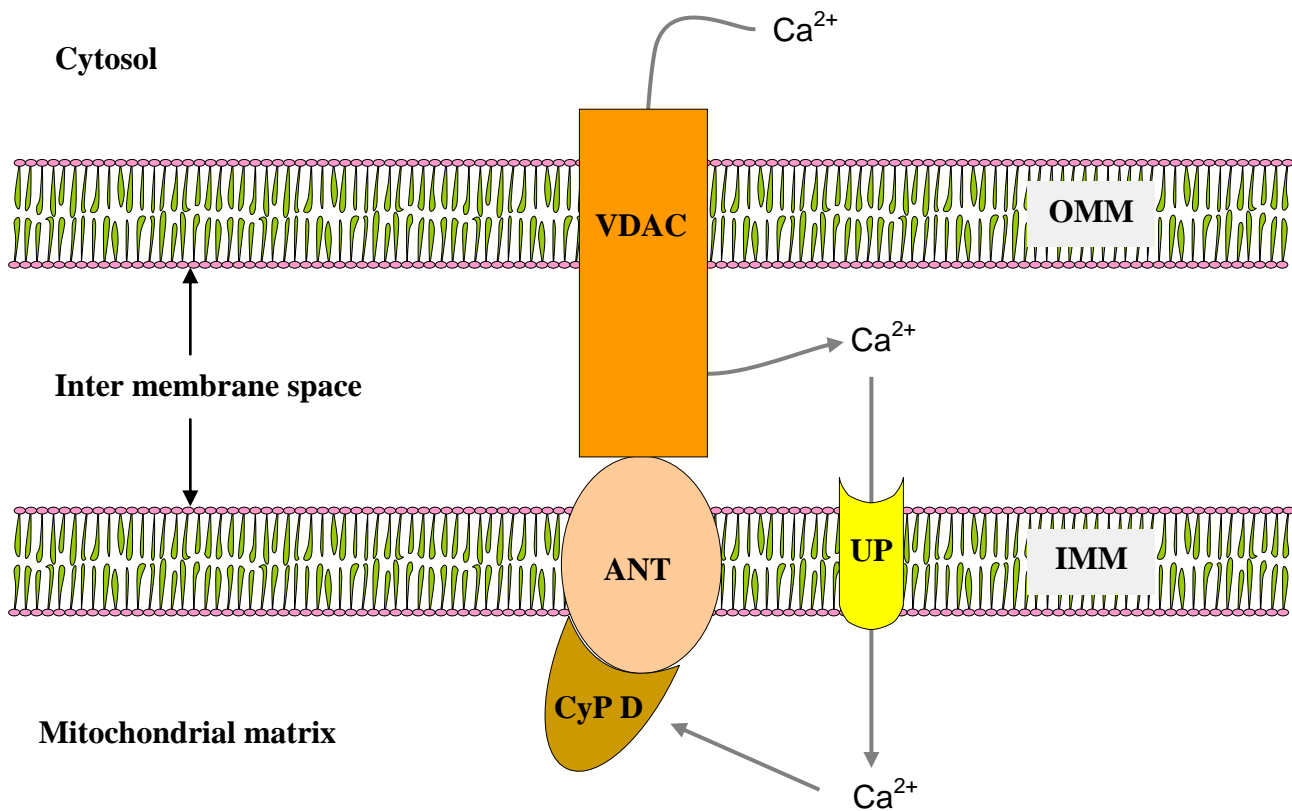

Figure 3: The components of the mtPTP and the dynamics of calcium uptake in the mitochondria (figure modified according to Crompton, 1999). OMM, outer mitochondrial membrane; IMM, inner mitochondrial membrane; VDAC, voltage gated anionic channel; ANT, adenine nucleotide translocase; Cyp D, cyclophilin D; UP, calcium uniporter.

when the Ca^{2+} release from the ER/SR is enhanced or is coincident with sensitization of the mtPTP (Hajnoczky et al., 2006). Recent studies have also shown that several pro-apoptotic factors, including members of the Bcl-2 family proteins and ROS regulate the Ca^{2+} sensitivity of both the Ca^{2+} release channels in the ER and the mtPTP in the mitochondria (Mathai et al., 2005). The loss of the balance between plasma membrane Ca^{2+} influx and Ca^{2+} export leads to a sustained elevation in cytosolic Ca^{2+} from 100 nM to ≥ 1 μM, inducing a progressive increase in mitochondrial Ca^{2+} uptake. When large quantities of Ca^{2+} are accumulated in the mitochondrial matrix, Ca^{2+} interacts with cyclophilin D to induce opening of the mtPTP (Basso et al., 2005). Furthermore, the rise in mitochondrial Ca^{2+} stimulates the generation of factors, including ROS and free fatty acids, which also promote the opening of the mtPTP (Starkov et al., 2004; Scorrano et al., 2001). Opening of the mtPTP causes dissipation of the mitochondrial membrane potential ($\Delta\Psi_m$) and release of Ca^{2+}. If the cytoplasmic Ca^{2+} overload persists, the mtPTP stays open and allows accumulation of solutes in the mitochondrial matrix. This in turn, leads to expansion of the matrix space and to rupture of the OMM, giving rise to release of the intermembrane space content (Green and Kroemer 2004). The formation of the pore leads to permeabilization and release of pro-apoptotic proteins from the mitochondria to the cytosol. Finally, impairment of the mitochondrial function and activation of cytoplasmic mechanisms by the released mitochondrial factors lead to execution of the cell.

1.4 Minocycline as a potentially protective drug

Minocycline (Figure 4) is a semi-synthetic second generation tetracycline antibiotic. It is effective against both, gram negative and gram positive infections and has been in use for over four decades with an acceptable safety profile. Because of its lipophilic nature, the bioavailability of this drug in the central nervous system is quite high, and it has been shown apart from its antimicrobial actions, to be effective in various models of neurodegenerative disorders like Parkinson's disease (Du et al., 2001; Wu et al., 2002), Huntington's disease (Chen et al., 2000), spinal cord injury (Yune et al 2007; Festoff et al., 2006) and ALS (Yong et al., 2004). The first neuroprotective effect of minocycline was observed in models of global and focal cerebral ischemia (Yrjanheikki et al., 1998 and 1999) and traumatic brain injury (Sanchez et al., 2001). Currently minocycline is under clinical investigation for stroke (Lampl et al., 2007), spinal cord injury (Fehlings and Baptiste, 2005), ALS (Pontieri et al.,

2005; Gordon et al., 2007), Huntington's disease (Bonelli et al., 2004), and Parkinson's disease (NET-PD, 2006). Although there are contradictory or inconclusive results, minocycline still remains one of the most interesting potential neuro-pharmaceuticals for clinical trials because of its broad spectrum of protective actions and good tolerability (Gordon et al., 2007; Keilhoff et al., 2007; Mievis et al., 2007; Fernendez-Gomez et al., 2005b).

The two mechanisms of action of minocycline as a neuroprotective agent are mainly postulated to be due to its anti-inflammatory and anti-apoptotic properties. The drug has anti-inflammatory effects attenuating ischemic injuries, endogenous IgG exudation, and the accumulation of neutrophils and macrophage/microglia. In addition, it also inhibits 5-LOX (lipooxigenase) expression and the production of leukotrienes (Chu et al., 2007). It has been shown to benefit in spinal cord injury by virtue of its anti-inflammatory property and inhibiting microglial activation (Festoff et al., 2006; Beattie, 2004). The anti-inflammatory effect of the drug has also been demonstrated in humans by its benefit in rheumatoid arthritis (O'Dell et al., 2001). Besides these effects, minocycline also possesses anti-oxidant properties (Kraus et al., 2005) and inhibition of neutrophil–mediated tissue injury by inhibiting neutrophil migration and suppressing formation of oxygen radicals (Elewa et al., 2006; Gaber et al., 1991). It was also shown to be a scavenger of peroxynitrite (Whiteman and Halliwell, 1997). Minocycline also inhibits the release of nitric oxide most probably by suppressing the expression of nitric oxide synthase (Amin et al., 1996; Lee et al., 2004).

Recently the protective effect of minocycline has been suggested to involve the mitochondrial dependent pathway. The anti-apoptotic effect of minocycline was observed in superoxide dismutase 1 mutant mice, where it delayed the progress of ALS like syndrome
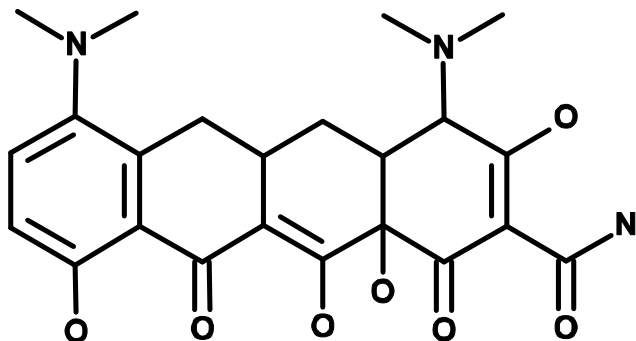

Figure 4: Chemical structure of minocycline

and also inhibited the release of cytochrome c from the mitochondria, both *in vivo* and *in vitro* (Zhu et al., 2002). It inhibits both, caspase-dependent and caspase-independent mitochondrial cell death and release of mitochondrial pro-apoptotic proteins (cytochrome c and SMAC / DIABLO) in Huntington striatal-cell model (Wang et al., 2003). An upregulation of Bcl-2 expression by minocycline and the abolishment of its anti-apoptotic action by Bcl-2 antisense was also reported (Wang et al., 2004). Furthermore, it blocks the release of cytochrome c in polyglutamine induced cell death in striatal neurone cell lines and influences the swelling induced by calcium. Other than interfering with mitochondrial apoptotic pathways minocycline has been shown to exert its protective effects in various CNS disorders by virtue of its antioxidant properties (Jordan et al., 2007), its anti-inflammatory effects (Stirling et al., 2004; Tomas-Camardiel et al., 2004), modulation of intracellular pathways such as PI3K/Akt (Pi et al., 2007), and mitogen-activated protein kinases (MAPK) (Wei et al., 2005; Tikka and Koistinaho 2001). Possible pharmacological application of minocycline in LHON has not been reported so far. Studying in a cybrid cell model of LHON disorder, the effects of minocycline on parameters of mitochondrial mediated cellular degeneration induced by thapsigargin (TG) can provide an initial glimpse of possible intervention for the disease.

1.5 Aim of the study

The neurodegeneration in LHON disorder is associated, in effect of complex I dysfunction, with high oxidative stress and energy metabolism imbalance (Qi et al., 2007a; Floreani et al., 2005; Zanna et al., 2005; Battisti et al., 2004; Ghelli et al., 2003; Zanna et al., 2003). Investigations for a treatment or pharmacological intervention of the disease, however, are infrequently put under focus. Our hypothesis is that under the biochemical circumstances due to the mutation causing LHON disorder, cell death can occur through mitochondrial pathways involving the mtPTP. The mtDNA mutation in LHON and its metabolic consequence provides an ideal circumstance for mtPTP to be formed under stressful conditions, which would lead to cell death by either caspase-dependent or caspase-independent apoptosis. Main objectives included:

1. To investigate the involvement of mitochondrial permeability transition in a cell death model of LHON cybrids

2. Establishing a cell culture based model for LHON as a pharmacological tool for initial drug screening

3. Devising pharmacological intervention to prevent cell death in LHON cybrids

4. Investigating possible effectiveness of antioxidants and mtPTP blockers in treatment of LHON

For the above stated objectives, we induced a calcium deregulation in the LHON cybrids using thapsigargin to provoke the opening of the mtPTP, and investigated the effect of minocycline (Figure 5). Minocycline was chosen for the study because it has been demonstrated to be an effective anti-apoptotic, anti-oxidant agent, and an effective neuroprotective in a variety of neurodegenerative disease models, in animals as well as in humans, and therefore qualifies as a good candidate to test in LHON disorder.
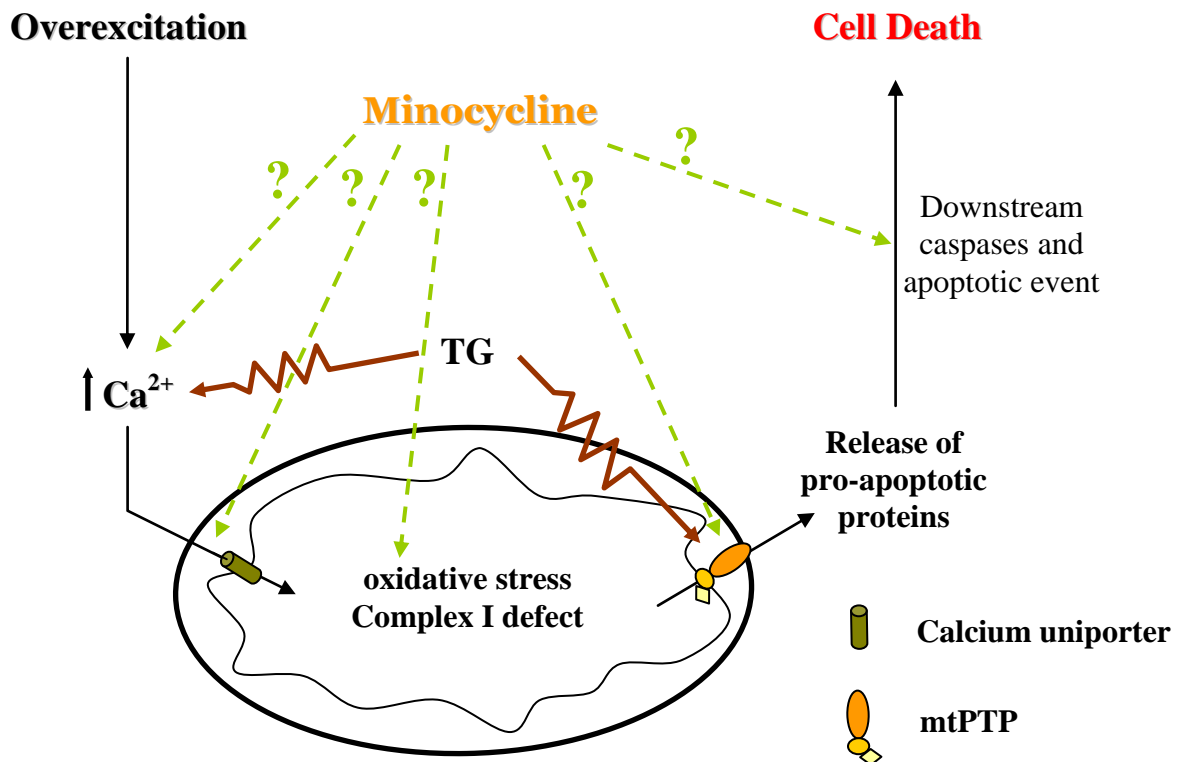

Figure 5: Diagram representing working hypothesis of the model and possible protective action of minocycline.

2.   MATERIALS AND METHODS

2.1 Chemicals, cell lines and culturing media

All chemicals enlisted in Table 1 were handled and stored as described by the manufacturer's protocol.

Table 1: Used chemicals and corresponding suppliers

Chemicals	Firm / company
• Active-caspase-3 antibody	Epitomics
• AIF antibody Rabbit monoclonal [E20]	Abcam
• ATP Bioluminescence Assay Kit CLS II	Roche
• Bicinchoninic acid (BCA) method kit for protein measurement	Pierce Biotech
• Bovine Serum Albumin	PAA
• Caspase-3 antibody H-277:(sc-7148)	Santa Cruz Biotech
• cyclosporin A (CsA)	Alexis
• cyclosporin H (CsH)	LKT labs
• Dulbecco's modified Eagle's medium (DMEM)	Sigma
• DMSO	Merck
• Foetal calf serum	PAA Laboratories
• Formaldehyde (for formalin solution)	Merck
• Goat Serum	PAN
• Goat anti Rabbit secondary Antibody – Alexa 488	Molecular Probes
• Fura-PE3-AM	Sigma
• H_2DFFDA (5-(and-6)-carboxy-2',7'-difluorodihydrofluorescein diacetate)	Molecular Probes
• Immu-Mount	Thermo Scientific
• L - glutamine.	PAA Laboratories
• Minocycline	Sigma
• Mitotracker green,	Molecular Probes
• Mitotracker Orange	Molecular Probes
• MTT (methylthiazolyldiphenyl-tetrazolium bromide)	Sigma

Chemicals (cont.)	Firm / company
• penicillin/streptomycin	PAA Laboratories
• pluronic acid	MobiTec
• protease inhibitor cocktail (Complete mini)	Roche
• Roti®Load1	Roth GmbH
• Sodium Azide	Serva
• Sodium pyruvate	PAA Laboratories
• Thapsigargin	Molecular Probes
• TMRM (tetramethyl rhodamine methyl ester)	Molecular Probes
• Triton	Ferak
• Uridine	Sigma
• Z-VAD-FMK	MBL international

2.1.1 Thapsigargin

Thapsigargin (TG, Figure 6) is a specific inhibitor of smooth endoplasmic reticulum (ER) Ca^{2+} ATPase (SERCA) and an important tool for studying Ca^{2+} stores. High concentrations of TG affect mitochondrial functioning, induce Ca^{2+} efflux and sensitize mitochondria to agents and conditions which induce permeability transition (Vercesi et.al, 1993; Hoek et.al, 1997). It has been assumed that TG promotes mitochondrial permeability transition by increasing the cytosolic calcium and therefore enhancing the mitochondrial matrix Ca^{2+} thereby increasing the sensitivity of the cell to undergo apoptosis. However, Korge et al. showed that the induction of MPT by TG can also be a result of a direct action not involving the increase of cytosolic calcium (Korge and Weiss, 1999).
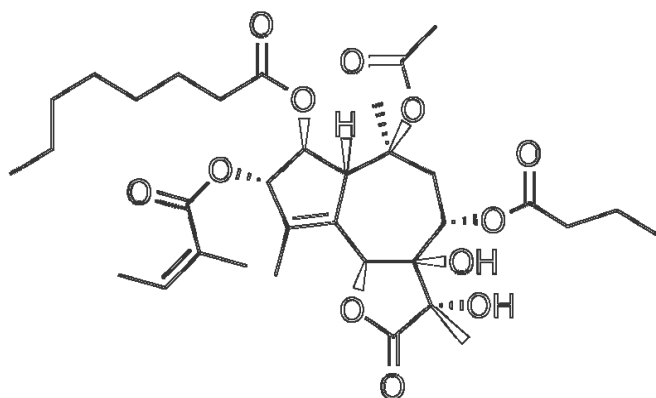

Figure 6: Chemical structure of Thapsigargin

The release of Ca^{2+} from the endoplasmic stores accounts for its most popular use. This however is achieved indirectly by preventing the pumps from counterbalancing the passive Ca^{2+} leak from the stores to the cytosol. Thus an appreciable rate of calcium leak, in addition to the presence of thapsigargin sensitive SERCA, is required for its action. If under a certain set of experimental condition, where the calcium leak is slow, on the time scale the peak Ca^{2+} spikes are not being achieved, the Ca^{2+} release can be afforded by calcium releasing agents (IP_3, caffeine, acetylcholine etc).

2.1.2 Cyclosporin A

Besides its immunosuppressive action cyclosporin A (CsA, Figure 7) is considered as a potent inhibitor of the permeability transition pore compared with Mg^{++} and ADP (Zoratti and Szabo et al., 1995; Broeckemeier et al., 1989). CsA by interacting with cyclophilin (the inner component of the pore) prevents its translocation to ANT (adenine nucleotide translocase) and eventually inhibits the formation of the lethal pore (Nicolli et al., 1996). In liver and heart mitochondria CsA protection depends on the extent and magnitude of Ca^{2+} loading and the presence of external Mg^{++} (Bernardi et al., 1992). CsA has been used to identify the activation of the mtPTP as a crucial factor leading to apoptosis and cell death (Zamzami et al., 1996). As a neuroprotective CsA ameliorates mitochondrial depolarization suggesting mtPTP involvement in excitotoxicity (Nieminen et al., 1996; Schinder et al., 1996; Vergun et al., 1999). It is one of the most frequently used research tool for studying mtPTP.
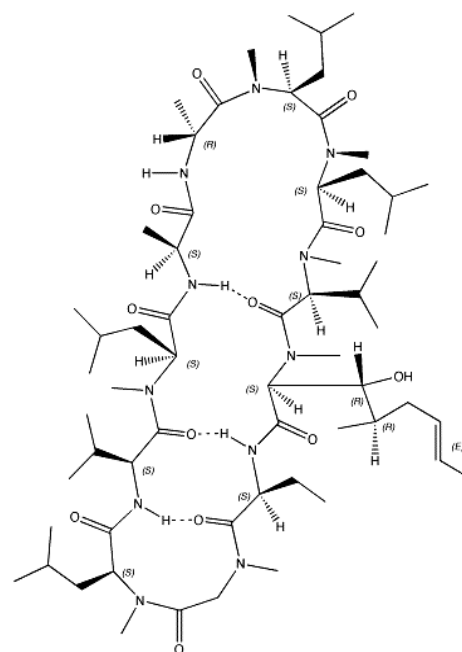
Figure 7: Chemical structure of Cyclosporin A

2.2 Cell lines and Culturing

NT2/D1 human teratoma derived cell lines were used as the parental controls and were obtained from ATCC (American Type Culture Collection). Cybrid cells with a G to A point mutation at the 11778 base pair of the mitochondrial DNA (which affects the amino

acid sequence of the ND4 subunit of complex I in the respiratory chain) were used as the LHON disorder model. The cybrid cell line was a generous gift from G. A. Cortopassi (Department of Molecular Biosciences, University of California Davis, Davis, CA 95616, USA). All cells were stored in a cryogenic solution under liquid nitrogen.11778 LHON cybrid cells and NT2 cells were cultivated in DMEM (high glucose, D 5648- Sigma). For propagation, cells were washed once with PBS, trypsinized and suspended in the culture medium. The suspension was spun down in a centrifuge at 1500 rcf for 5 minutes and the pellet re-suspended in fresh medium. The cell density in the suspension was counted with a Neubauer chamber and cells were plated at the required density (approximately 10^5 cells per ml) in incubating flasks or onto sterile glass coverslips. In both the cell lines, treatments with minocycline or CsA were done 30 minutes prior to instillation of thapsigargin.

2.2.1 Culturing media and buffers

Culturing media (1L)

- DMEM (high glucose, D 5648- Sigma) 13.4 g/L
- Sodium pyruvate 110 mg/l
- $NaHCO_3$ 1.5 g/l
- Foetal calf serum 100 ml/l
- Uridine 50 mg/l
- L-glutamine (200mM) 10 ml/l
- Penicillin (10 units/ml) / streptomycin (10 µg/ml)
- Distilled water adjusted until 1 liter

The mixture was sterile filtered, stored at 4°C and used within 1 month from the day of reconstitution.

PBS

- $Na_2HPO_3 \bullet 12\ H_2O$ 295 mg/l
- KH_2PO_4 240 mg/l
- KCl 200 mg/l
- NaCl 8 g/l
- Distilled water up to 1 liter

pH adjusted to 7.4 with HCl

TBS

- Tris 24.2 g/l
- Nacl 80 g/l

PH was adjusted to 7.6 with HCl

HBSS solution

- NaCl 8,006 g/l
- KCl 373 mg/l
- $CaCl_2$ 205 mg/l
- Glucose 991 mg/l
- Hepes 4.76 g/l
- KH_2PO_4 81 mg/l
- K_2HPO_4 10.45 mg/l
- $NaHCO_3$ 840 mg/l
- $MgCl_2$ 182 mg/l

pH was adjusted to 7.4 with NaOH

2.2.2 Poly-D-lysine coating

For better adherence of cells to the plastic or glass surfaces coated with Poly-D-lysine (PDL) were used. Each sterile coverslip were first kept in a sterile Petri dish and mounted with a 1 ml drop of PDL solution (0.1 % solution of poly-D-lysine was prepared by dissolving 1 mg of poly-D-lysine in 1 ml of 0.15 M boric acid prepared in PBS) at the centre of the coverslip such that the drop covers the whole area of the coverslip without running onto the Petri dish. The coverslips along with the PDL solution were then kept at room temperature under a sterile laminar flow hood for 1 hour. Finally, the droplets were sucked off and the coverslips washed once with sterile water. PDL coatings were kept in a sterile incubator and could be used 24 hours later.

2.3 Cell viability assay

A colorimetric test, methylthiazolyldiphenyl-tetrazolium bromide (MTT) reduction assay was used to assess cell viability. This homogeneous colorimetric assay is based on the conversion of the tetrazolium salt MTT, a pale yellow substrate, to formazan, a purple dye (Figure 8). This cellular reduction reaction involves the pyridine nucleotide cofactors NADH/NADPH and is only catalyzed by living cells. The formazan product has a low aqueous solubility and is present as purple crystals. Dissolving the resulting formazan with a solubilization buffer permits the convenient quantification of product formation. The intensity of the product color, measured at 550 - 620 nm, is directly proportional to the number of living cells in the culture.
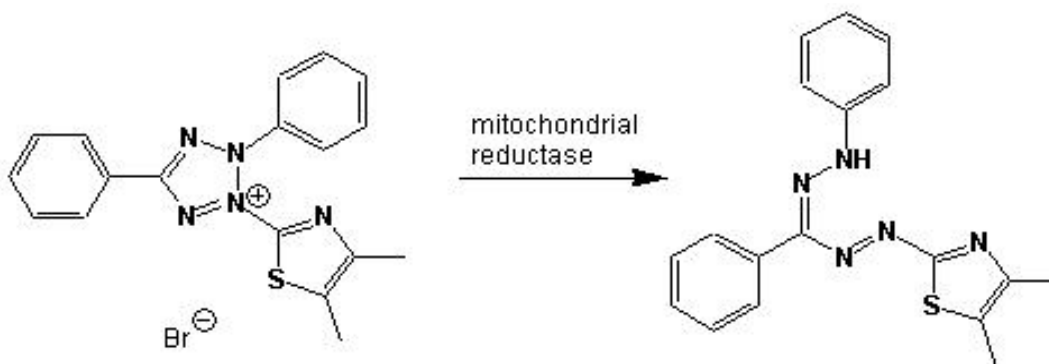
Figure 8: MTT reduction to formazan

LHON cybrid cells and NT2 cells were grown in a 24 well plate (approximately 5×10^4 cells per well) for 24 hours before an apoptotic stimulus with TG was given for a duration of 12 hours. A dose response curve of thapsigargin at concentrations of 100 nM, 500 nM, 1 µM, 2.5 µM, and 5 µM was plotted to establish the LD_{50} of the same. In another experiment a general caspase inhibitor, z-VAD-FMK, was used to establish the nature of cell death. Treated groups (n=12 in each case) were incubated with the drug 30 minutes prior to the apoptotic stimulus. After incubation the medium was replaced by 0.5 ml of 1 mg/ml MTT solution in sterile PBS for 1 hour. The formazan formed by the mitochondria of viable cells was then dissolved in DMSO (dimethyl sulphoxide) and the optical density of the solution measured on an ELISA plate reader at 570 nm. Cultures were tested for the survival of cells with different concentrations of minocycline (50, 75, 100, 125, 150, and

200 µM) and CsA (1, 2, 3, and 5 µM) against TG-induced apoptosis. The percentage survival was calculated by taking the arithmetic mean of control values as reference.

2.4 DAPI staining

Specific fluorescent staining of the nuclei was done using DAPI (4',6-Diamidine-2-phenylindole dihydrochloride). The dye binds selectively to DNA and forms strongly fluorescent DNA-DAPI complexes with high specificity. On adding DAPI to cell culture it is rapidly taken up into cellular DNA yielding highly fluorescent nuclei and no detectable cytoplasmic fluorescence. If the cells are apoptotic a characteristic nuclear condensation can readily be detected.

Working solution of DAPI was used as 1 µg/ml dissolved in methanol. The cells were plated on the PDL coated coverslips at an approximate density of 2×10^5 and allowed to grow for 32 hours. Cells were then treated with thapsigargin for 8 hours, washed with PBS and methanol after which they were incubated with the working solution of the dye for 15 minutes at 37°C. The coverslips were then washed with methanol and mounted onto the slides. The slides were left out to dry overnight. Axiophot fluorescence microscope (Karl Zeiss) was used to image the nuclear morphology in both cell lines with and without thapsigargin treatment.

2.5 Immunocytochemistry

Immunocytochemistry was done to visualize the release of AIF from the mitochondria and its translocation to the nucleus. After incubating the cells with thapsigargin the coverslips were incubated with 40 nM Mitotracker Orange for 30 minutes at 37°C in HEPES buffer and thereof fixed with 4% formalin for 30 minutes. The coverslips were then washed 3 times with PBS solution for 10 minutes each. The culture was blocked with 10% serum and incubated overnight at 4°C with the primary AIF antibody diluted (1:500) in 10% serum containing 0.3% Triton and 0.1% sodium azide. The next day 3 times washing with PBS was given, after which the culture were again blocked with Bovine serum albumin (BSA) in PBS for 30 minutes. Cells were then incubated with the anti-rabbit-Alexa488

conjugated secondary antibody diluted (1:500) in 0.2 % BSA in PBS for 4 hours in the dark at 37 °C or overnight at 4 °C, after which thrice washing with PBS was given. For labelling the nucleus of the cells the same were then incubated with DAPI as explained in the DAPI staining protocol above. Finally the coverslips were mounted onto the slides with a mounting solution and stored at 4 °C protected from light.

The slides were imaged with Zeiss Axiophot fluorescence microscope with green (BP 546 nm), blue (BP 450 nm – 490 nm) and ultra violet (BP 365 nm) filters corresponding to mitotracker Orange, Alexa 488 complex, and DAPI staining, respectively. The pictures were taken with an Axiocam using Axiovision software.

2.6 ATP measurements

ATP measurement was performed using a bioluminescence ATP assay kit (ATP assay Kit CLS II, Roche). According to the manufacturer's protocol, the ATP dependency of the light emitting luciferase catalyzed oxidation of luciferin was used for the measurement of extremely low concentrations of ATP.

Standard curve

ATP standards were appropriately diluted to give the following dilutions:

1 µM ATP

0.5 µM ATP

0.25 µM ATP

0.125 µM ATP

0.0625 µM ATP

The standard curve was plotted and was subjected to regression analysis.

ATP measurement buffer

- Tris 12.114g/l
- EDTA 1.169 g/l

pH adjusted to 7.75

Samples were collected from both NT2 cell line and LHON cybrids at 1, 1.5, and 2 hours after incubation with thapsigargin. The effect of minocycline was also studied in this model to observe changes, if any, on the ATP levels under the influence of the drug.

Cells were trypsinized and spun down at 1000 g for 5 minutes. The supernatant was discarded and the pellet re-suspended in PBS. The cells were again centrifuged at 1000 g for 2 minutes, the supernatant replaced with boiling ATP measurement buffer, and incubated for another 2 minutes at 100 ºC. Samples were centrifuged at 1000 g for 1 minute and the supernatant was transferred to a fresh tube. An appropriate dilution of the supernatant was then mixed with luciferase reagent and measured for luminescence intensity using a TD-20/20 luminometer. The calibrated luminescence and regression of the standards was applied to get the ATP concentrations from the sample readouts. These values were then adjusted to the protein level of the samples.

2.7 Calcium imaging

Cells were cultured on sterile coverslips and visualized for live cell imaging 32-48 hours later. Fura-PE3-AM with an end concentration of 5 μM was used as fluorescent ratiometric calcium indicator (stock solution prepared in a 20 % pluronic acid in DMSO). Microscopy was done with Meta Fluor software on the Zeiss Axiovert 100M Pascal confocal microscope with Visitron Systems GmbH setup. The ratiometric imaging required the use of two wavelengths (340 nm and 380 nm). At absorption wavelength of 340 nm the dye's fluorescence intensity increases as the amount of Ca^{2+} binding to the dye increases.
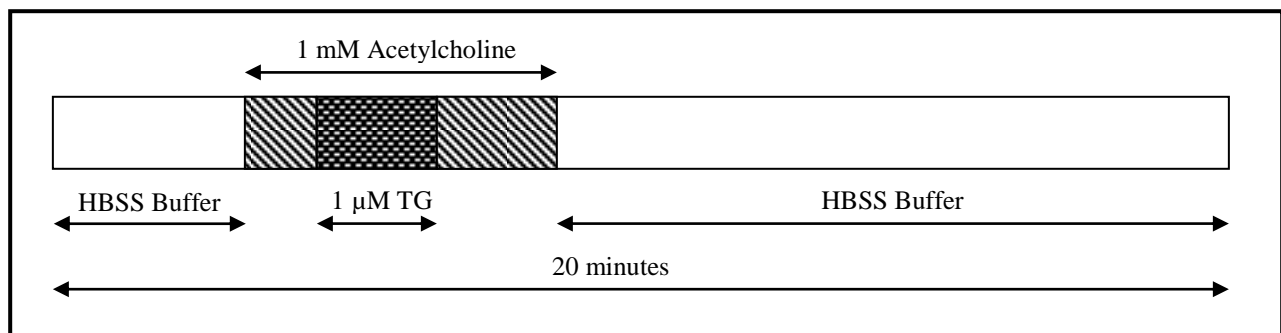

Figure 9: A schematic diagram of calcium imaging experiment. Treatments with minocycline and CsA are given 30 minutes prior to imaging and throughout the perfusion.

On the other hand the inherent fluorescent intensity of the dye increases with decrease in the binding of Ca^{2+} if the incident wavelength is 380 nm. The fluorescent ratio of 340 nm/380 nm therefore amplifies the signal of calcium within the cell. Cells were incubated with the dye at a concentration of 5 µM for 30 minutes. After the incubation the cells were washed with HBSS once to drain away excess dye. The coverslips were then placed in a fixed chamber and mounted on a thermostatic metallic grid (maintained at 37 ℃) on the microscope and perfused with HBSS at 37 ℃ with or without the drug investigated. For evaluating the effects of minocycline and CsA the cultures were incubated with the respective drug for 30 minutes prior to the commencement of the experiment. At the beginning of the experiment, buffer was perfused through the culture for 3 minutes to get a stable baseline after which the experimental recording was started. The optimized experimental setup is schemed in Figure 9. Acetylcholine was used to induce calcium release after which TG at a concentration of 1 µM was perfused to completely and irreversibly inhibit the reuptake of calcium back to the endoplasmic stores. The change in the cellular calcium was measured by the ratio of the two fluorescent intensities at 340 nm and 380 nm, which corresponds to the calcium bound and the native form of the dye, respectively.

2.8 Mitochondrial depolarization

Cells were cultured on Poly-D-lysine coated coverslips for 24 hours and mitochondrial depolarizing experiments were conducted in cell culture medium which was deficient in serum. Tetramethyl rhodamine methyl ester (TMRM, at an end concentration of 100 nM, stock solution prepared in a 20 % pluronic acid in DMSO) was used to assess the mitochondrial depolarization after TG-induced apoptosis, and Mitotracker Green (at an end concentration of 160 nM, stock solution prepared in a 20 % pluronic acid in DMSO) for simultaneously visualizing the total population of mitochondria. After eight hours of incubation with 1 µM TG, with or without 100 µM minocycline or 3 µM CsA, the coverslips were incubated with Mitotracker Green and TMRM for 30 minutes and 15 minutes respectively, and view fields were selected randomly for taking pictures with the Zeiss Axiovert 100M Pascal confocal microscope. Cells from different coverslips were counted for those stained with mitotracker green (total number of cells) and for those that were additionally stained with TMRM (cells with conserved mitochondrial membrane

potential). From each treatment group (n = 5-6) at least 4 pictures were taken and pooled for analysis. Percentage of cells with intact mitochondrial membrane potential was calculated by dividing the number of TMRM stained cells by the total number of cells stained with Mitotracker Green.

2.9 Protein determination

For western blotting protein measurement was performed by using commercially available kit (BCA^{TM} protein assay kit, Pierce) based on the bicinchoninic acid (BCA) method (Smith et al., 1985). 20 µl of the sample or standard was mixed with 1ml of working solution and kept at room temperature for 30 minutes. The optical density of the solution was read at 570nm. Standard curve was constructed using standard solution of BSA at concentrations 100, 200, 400, 600, 800, 100, and 1200 mg/L. The regressed curve obtained by the standards was used as reference for the protein readout in the samples.

For ATP measurements Bio-Rad DC (detergent compatible) colorimetric protein assay was used. All regents were prepared according to the instructions of the manufacturer. The reaction is based on the well-documented Lowry assay (Lowry et al. 1951). The BioRad *DC* protein assay is measured at 650–750 nm with a standard laboratory spectrophotometer or microplate reader. The standard protein was in the form of BSA solutions with concentrations 0.0, 0.1, 0.25, 0.50, 1.0, 1.5, 2.0, and 3.0 mg/l. A standard curve was plotted with the help of regression and the protein concentrations of the samples were extrapolated.

2.10 Western blotting

The ratio of active-caspase-3 to pro-caspase-3 (aC3/pC3) was calculated by analysis of Western blots of LHON cybrid cells and the NT2 cell line subjected to TG-induced apoptosis. The time point of sample collection was 8 hours after incubation with 1 µM TG with or without treatments (n=5 cultures for each treatment). The cells were scraped and then spun down at 1500 g for 5 minutes. Pellets were re-suspended in 0.05 M sodium phosphate solution containing protease inhibitor cocktail and transferred to an Eppendorf

tube and spun again. The pellets were then homogenized with a Teflon tip homogenizer and spun again at 14000 rcf for 5 minutes. The supernatants obtained were taken for analysis.

Separation Gel buffer
- Tris 1.5 M
- SDS 0.4 %
- EDTA 2.9 %

pH adjusted to 8.8 with HCl

Collection Gel buffer
- Tris 0.5 M
- SDS 0.4 %
- EDTA 2.9 %

pH adjusted to 6.8 with HCl

Electrophoresis Buffer
- Tris 3.03 g/l
- Glycine 14.4 g/l
- SDS 1 g/l

Blotting buffer (2L)
- Tris Base 4.543 g
- Glycine 21.6 g
- SDS 4 ml of 10 % SDS solution
- Methanol 400 ml

Blocking solution

5 % solution of low fat Milk protein powder dissolved in TBST (TBS with 0.1 % Tween)

Gel was casted in a Hoeffer gel caster. Ten teeth comb was used to cast the wells in the loading gel with a sample volume of not more than 20 µl per well. Samples were first solubilized with a solubilizer (Roti®-load1).

Electrophoresis was done on gradient acrylamide gel (5-20%). Protein was then transferred onto a nirtrocellulose paper by wet blotting transfer with the help of a blotting apparatus at about 80 mA for 90 minutes. The blots were washed three times, five minutes each, and blocking was done for 4 hours at room temperature. Primary antibodies (Caspase-3 antibody was used with 1:200 dilution and active-caspase-3 antibody at a dilution 1:500) were incubated with the blot at 4ºC overnight, washed with PBS 3 times (each for 5 minutes) and incubated with horseradish peroxidase conjugated secondary antibody for 2 hours at room temperature. After a minute of contact with the reconstituted Western blotting detection reagents (ECL^{TM} Amersham) the blots were developed using a chemiluminescence film (Hyperfilm ECL^{TM}, Amersham). Band intensities of the blots obtained with Quantity one (1D analysis software from BioRad) were subjected to calculation of aC3/pC3 ratio. The ratios of normal untreated groups were normalized to a value of 1.

2.11 DFF imaging

5-(and-6)-carboxy-2',7'-difluorodihydrofluorescein diacetate (carboxy-H$_2$DFFDA) is a photo-stable congener of the widely used intracellular ROS detecting dye dichlorofluorescein (DCF) which fluoresces upon oxidation (Jakubowski and Bartosz, 2000). Experiments were performed on cells cultured on coverslips, incubated with the dye (stock solution prepared in a 20 % pluronic acid in DMSO) for 1 hour and the respective drugs for 30 minutes prior to imaging and mounted onto the confocal microscope in a thermostatic chamber. The medium was replaced with 990 µl of modified Locke's solution (7.58 g/l NaCl, 300 mg/l KCl, 240 mg/l CaCl$_2$, 240 mg/l MgSO$_4$, 340 mg/l NaHCO$_3$, 2.42 g/l HEPES , 1.82 g/l glucose, adjusted to pH 7.3) without and with different concentrations of the drug investigated. Fluorescence (excitation at 488 nm and emission at 530 nm) was measured in living cells using a Zeiss Axiovert 100 M Pascal confocal microscope for at least 10 minutes. Experimental settings including the pinhole diameter, intensity of the laser, and the detector gain was kept uniform in all the experiments performed. The first 100 seconds of the measurement were used to obtain a steady baseline after which 10 µl of 10 mM H$_2$O$_2$ solution in modified Locke's solution was injected into the monitored culture (final concentration of 100 µM H$_2$O$_2$). The regions of interest were

defined and the intensities of fluorescence were recorded from those particular areas. Analysis was conducted with subtraction of background intensities in respective cultures.

2.12 Statistical analysis

All results are expressed as mean ± S.E.M. A One-way ANOVA followed by Dunnett's t test was performed to assess the difference between and within the treatment groups in all experiments where more than two groups were planned for comparison. For the results obtained by calcium imaging, the fluorescent values were collected at a time point of every 100 seconds after the withdrawal of calcium stimulus. For this experiment, a two-way ANOVA was done to assess bi-factorial treatment × time effect. A p value of F statistics less than 0.05 indicates that at least one pair of the treatment groups differed significantly in the two-way ANOVA. Bonferroni's multiple comparison test was applied to test exactly which pair(s) of treatment significantly differed. Student's t- test was used to evaluate whether TG induced a significant difference in the aC3/pC3 ratio between the two cell lines. All statistical tests were done by using GraphPad Prism 4 (GraphPad Software).

3.   RESULTS

3.1 Minocycline and cyclosporine A protect LHON cybrids against TG induced toxicity

In the MTT assay the LD_{50} of thapsigargin in LHON cybrid cells was determined to be 1 µM. The dose caused significant decrease of surviving cybrids cells to below 50% shown as the encircled concentration (Figure 10). This concentration of TG was then taken in all the experiments performed thereon.
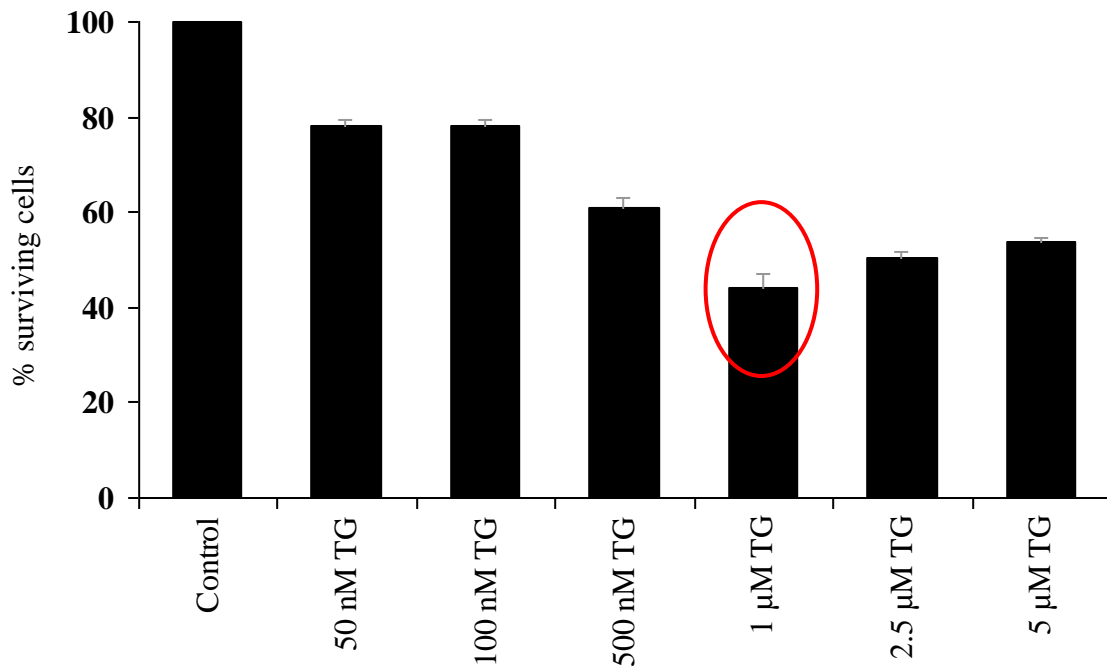
Figure 10: LD_{50} determination of TG in LHON cybrid cells using MTT assay.

In the cell viability assay TG significantly decreased the percentage of survival in both cell lines (In Figure 11A the viability in NT2 cell line was reduced to 71.7 ± 0.67 %, n=6, p<0.05 and in LHON cybrid to 49.5 ± 1.96 %, n=6, p<0.05; In Figure 11B the viability of NT2 cell line was reduced to 69.2 ± 0.73 %, n=6, p<0.05 and LHON cybrid to 53.7 ± 2.68 %, n=6, p<0.05). The difference in the survival rate of LHON verses NT2 cells treated with TG was significant which indicated that the LHON cybrids were more sensitive to the apoptotic stimulus. LHON cybrids with the same mutation, but based on the 143B TK (-)

osteosarcoma cell line, have previously been shown to be more sensitive towards apoptotic stimulus (Danielson et al., 2002). The concentration response curve shows for LHON cybrid cells that the treatment with minocycline at concentrations of 100-125 µM prevents apoptosis as indicated by a higher rate of survival (Figure 11A). A minimum effective dose
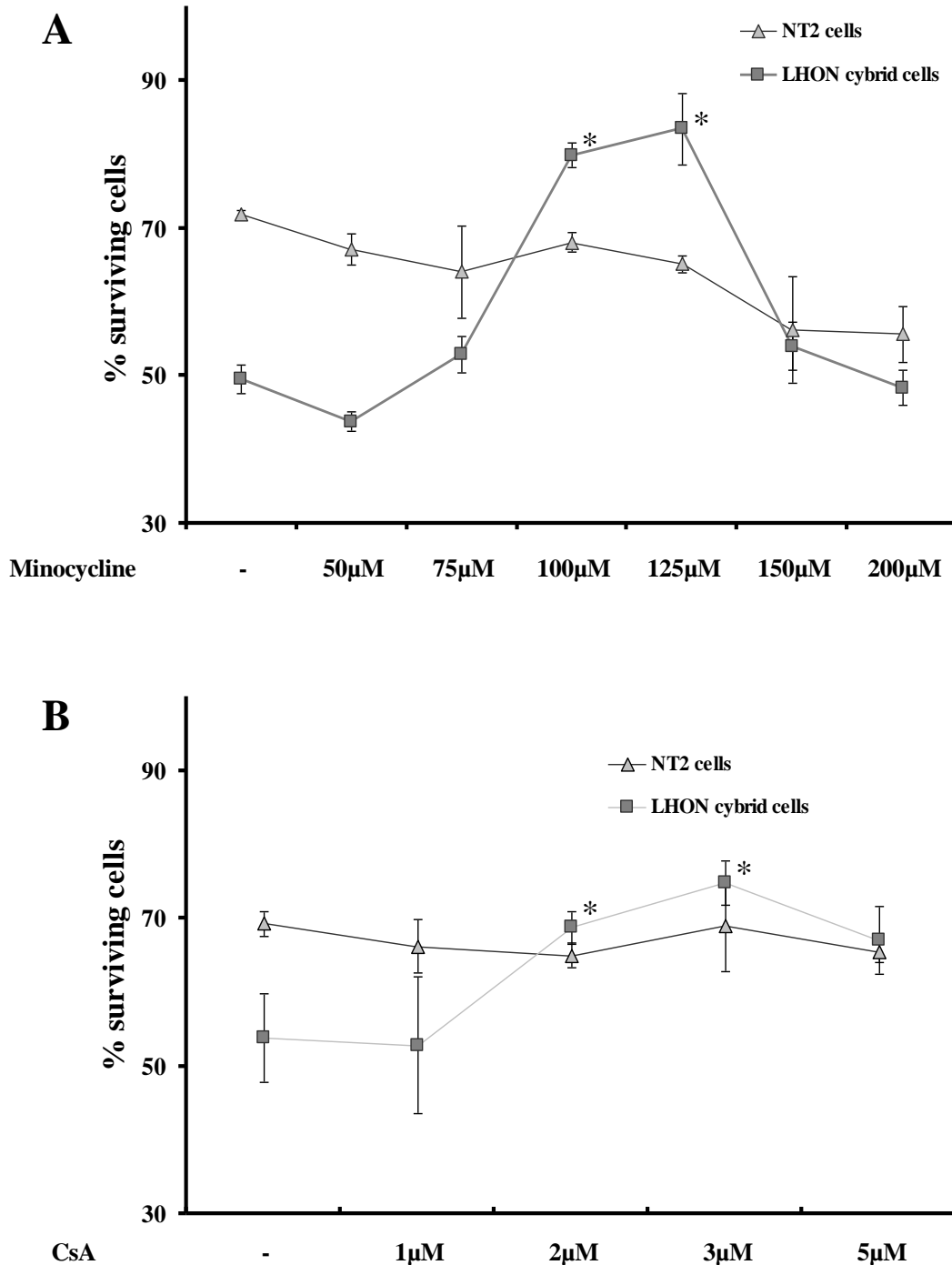

Figure 11: LHON cybrid and NT2 cell survival assay and concentration response curve of minocycline (A) and CsA (B) against TG-induced cell death. * p<0.01).

of minocycline in the LHON cybrid cells was found to be 100 µM (78.8 ± 1.72 %, p<0.05). At higher doses there was manifestation of toxic effects of minocycline because the percentage of survival significantly decreases to 53.9 ± 3.3 % and 48.3 ± 2.3 % respectively at doses 150 µM and 200 µM. On the other hand however, in the parental cell lines, the protective effect of minocycline was not observed at any concentration. Toxic effect of minocycline at concentrations of 150-200 µM, as seen in the cybrid cells, were observed in the NT2 cell line as well. Concentration response curve of CsA in the two cell lines (Figure 11B) showed that there is no significant increase in cell survival at any concentration in the NT2 cells whereas the minimum effective dose in the LHON cybrid cells was 2 µM (68.7 ± 0.95 %, p<0.05). In addition, 3 µM CsA (74.78 ± 1.31 %) shows a significantly higher protection than 2 µM CsA in cybrid cells.

In an additional experiment using a general caspase inhibitor z-VAD-FMK it was observed that neither cell line showed significant protection from TG induced decrease in cell viability when the general caspase inhibitor was present in the incubation media. LHON cybrids upon TG decreased to viability which remained unchallenged in presence of the general caspase inhibitor (Figure 12B). Similarly, NT2 cells showed a decrease in viability upon TG insult which was also unaltered by z-VAD-FMK treatment (Figure 12A). This suggests that the cell death induced by TG was not dependent on caspase activation. To validate the above stated results which suggest that apoptotic cell death is not the reason for the decrease in cell viability in the MTT assay we performed DAPI staining and activecaspase-3:procaspase-3 (aC3/pC3) Western blot of cells treated with TG to grant a further account for the decrease in cell viability in the MTT assay.
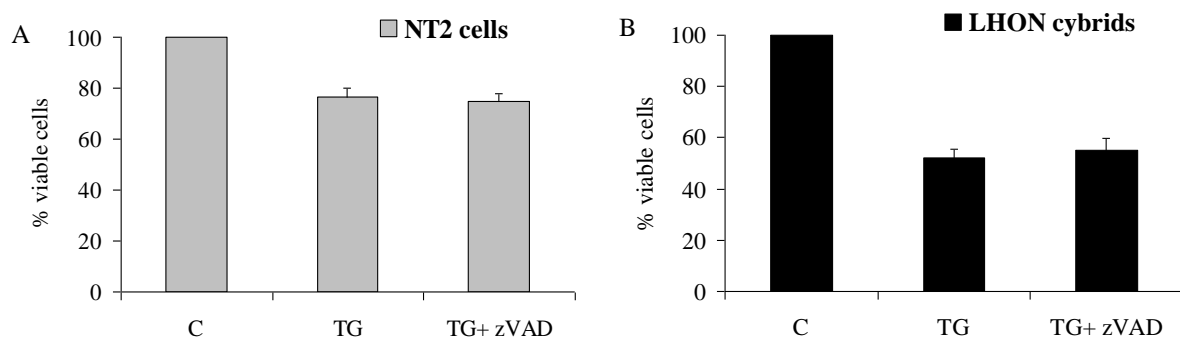
Figure 12: Cell viability assay of LHON cybrids and NT2 cells upon TG insult in presence of a general caspase inhibitor z-VAD-FMK

3.2 DAPI staining shows apoptotic nuclear morphology in TG treatment

DAPI binds selectively to DNA forming a DAPI-DNA complex. The staining is used widely to study the morphology of the nucleus. An apoptotic nucleus would be visible as a condensed bright kernel of the cell. After 8 hours of incubation with 1 µM thapsigargin DAPI staining performed in both cell line showed typical apoptotic morphology of their nucleus. Nuclear condensation was present throughout the culture (Figure 13). This was rather unexpected as the cell death indicated by the MTT assay was not considered apoptotic due to ineffectiveness of z-VAD-FMK to protect the cells.
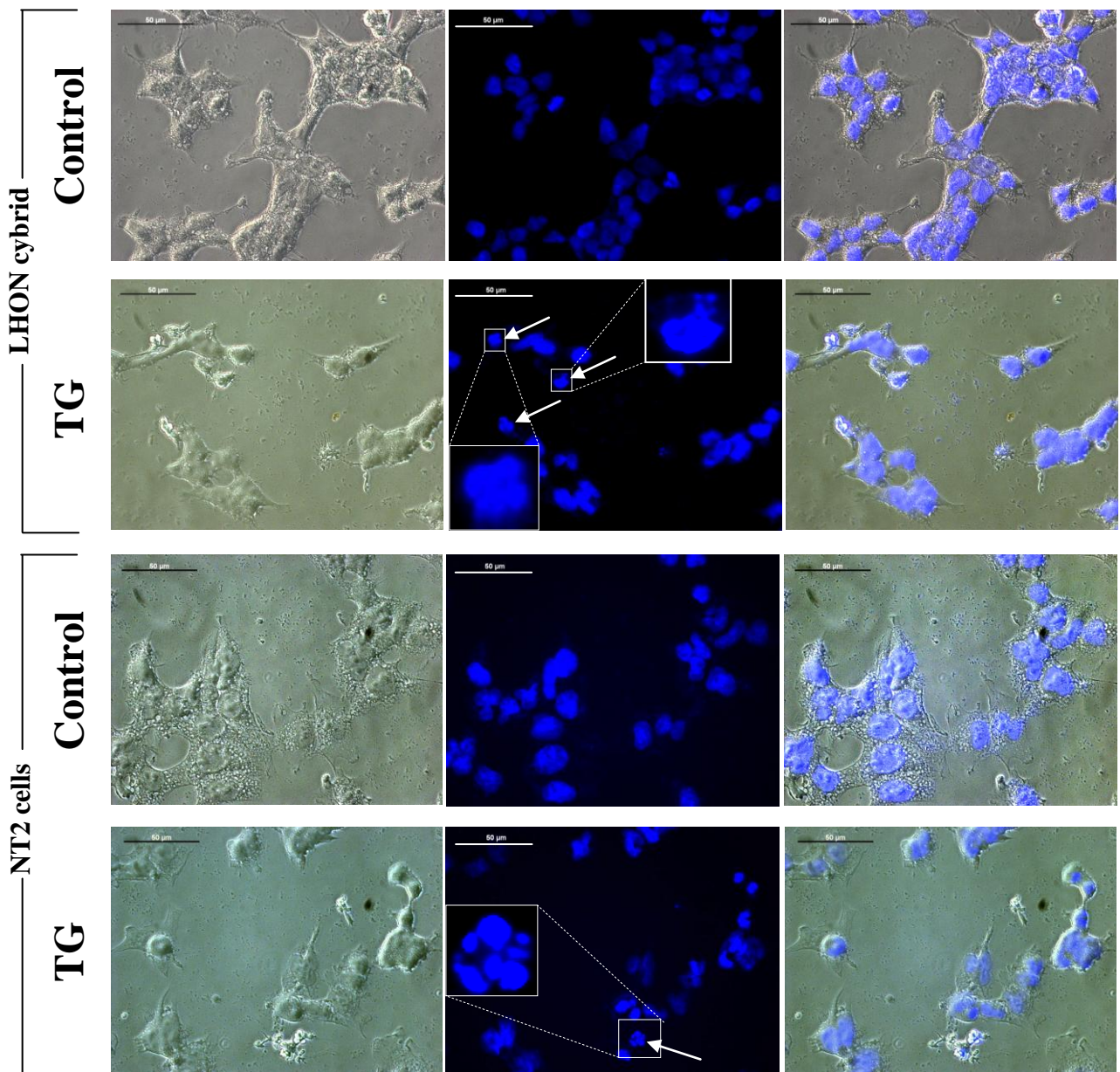
Figure 13: DAPI staining of NT2 and 11778 LHON cybrid cells shows distinctive nuclear condensation (white arrows) and apoptotic event in TG treatment. Scale bar of 50 µm applies to all pictures.

3.3 Apoptosis inducing factor translocates to the nucleus in TG treatment

AIF translocation constitutes a hallmark of permeability transition pore induced caspase independent apoptosis. As the cell death in our experiment turns out to be caspase independent but CsA sensitive, with DAPI staining showing signs of nuclear condensation, it is quite possible that AIF release constitutes the major pathway of apoptosis. The
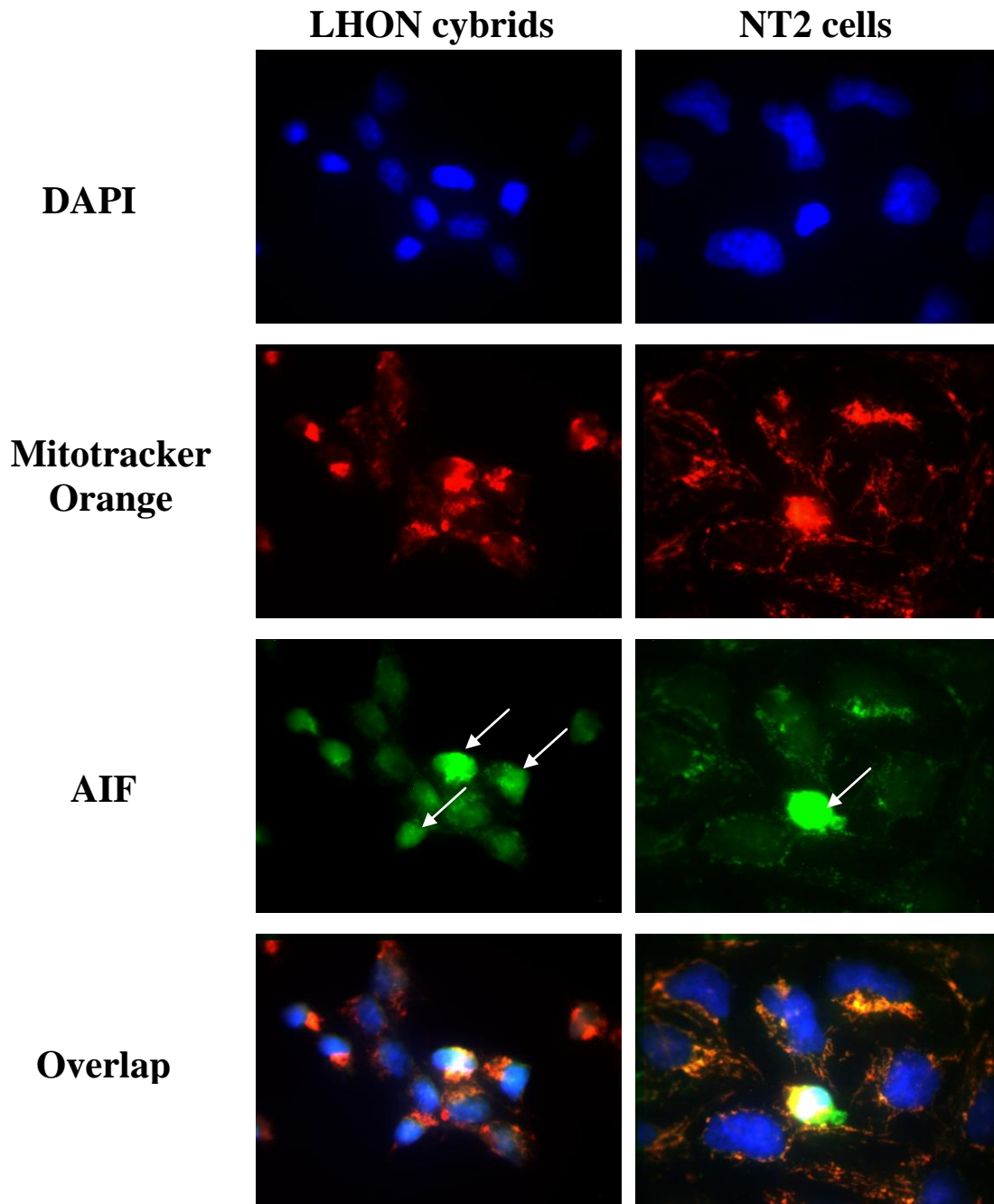
Figure 14: Immunocytochemistry of AIF shows its translocation to the nucleus upon TG treatment in both cell lines. White arrows indicate presence of AIF in nucleus.

immunocytochemistry did indeed show the same to be true. TG induced a translocation of AIF labeling from the mitochondria to the cytoplasm and nucleus (Figure 14). The triple labeling of AIF antibody, DAPI and mitotracker orange shows that TG treatment causes a release of AIF in LHON cybrids as well as in NT2 cells, the latter showing considerably lower number of cells with AIF translocation than the former. Due to the nature of simple fluorescence microscopy a heavy load of background is visible which is because this type of microscopy, unlike the confocal microscopy, does not measure fluorescence from a thin section of the sample culture (Figure 14).

3.4 Thapsigargin treatment decreases ATP levels in LHON cybrids

Since apoptosis is an energy dependent process, the level of ATP is a critical player. To observe the dynamics of cellular energy in our experimental model of TG induced cell death luminometric analysis of ATP was conducted at different intervals of TG treatments in both cell lines. The ATP levels of LHON cybrids initially decreased significantly but reclined at 2 hours of the treatment. The NT2 cells however did not show a significant decline in ATP level in any of the measurements performed after thapsigargin treatment.
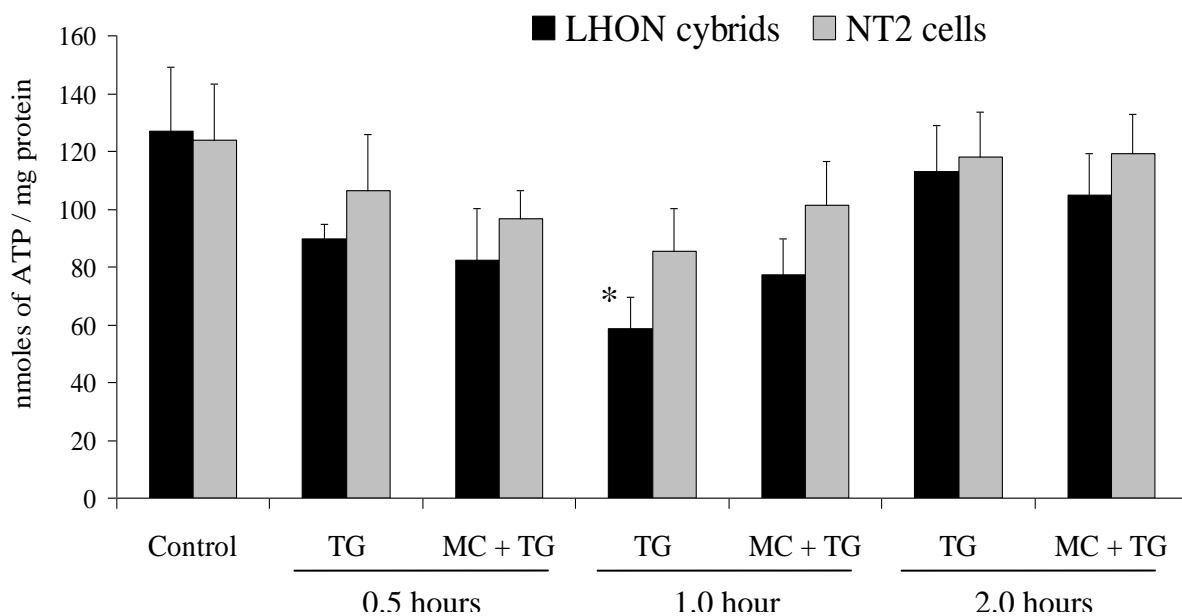
Figure 15: ATP measurements, with and without 100µM minocycline (MC), in LHON cybrids and NT2 cells treated with TG. A significant decline in ATP levels in the TG treated LHON cybrids is seen, but not in NT2 cells.

100 µM minocycline treatment failed to modify the ATP level changes brought by thapsigargin (Figure 15). A cytosolic calcium increase should ideally stimulate the respiratory production of ATP by enhancing the activity of calcium sensitive dehydrogenase and therefore increasing the production of H^+ ions. On the other hand, calcium itself being a cation can render the matrix more positive and decrease the membrane potential. This is well visible with NT2 cells where the decrease is insignificant. LHON cells, however, showed a decrease of ATP production with TG insult.

3.5 Minocycline and cyclosporine A alleviate calcium deregulation

Ca^{2+} as the centre of mitochondrial apoptotic research has been shown to undergo deregulation upon mtPTP opening (Andrabi et al., 2004). In the visitron imaging, cells can be seen as small island clusters which appear as dark patches and the background appears to have a higher fluorescence. This is a pseudo-background effect, as the small amount of dye

Figure 16: Pictorial representation of the LHON cybrid cells in a ratiometric calcium imaging experiment using Fura-PE3-AM. Both CsA and minocycline showed a lowering of the cellular levels of calcium after the withdrawal of the TG stimulus.

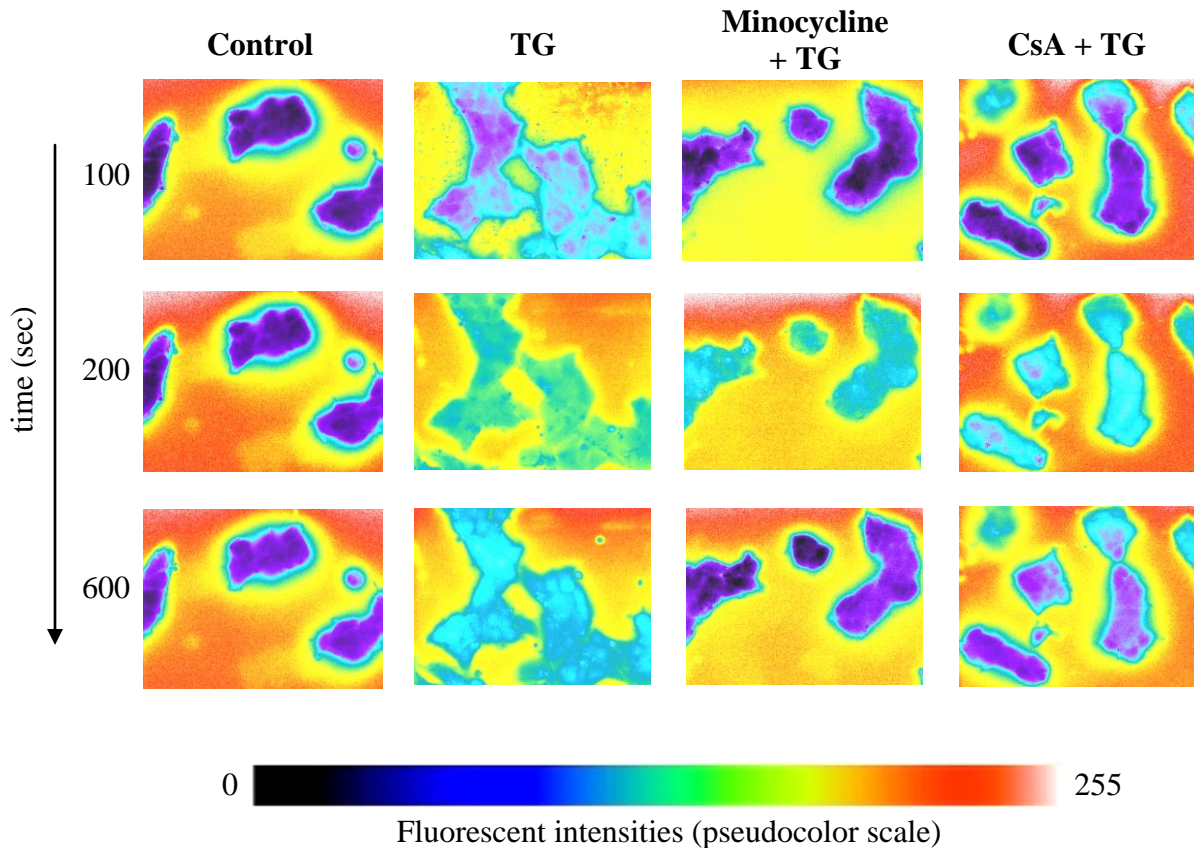leaking out of the cells bind to high extra-cellular calcium (present in the buffer) and gives out a false fluorescence ratio. The fluorescence ratios of the cell islands change without significant change in the background (Figure 16). Using ROIs on individual cells we conducted the live cell calcium imaging to visualize the calcium dynamics in our model of investigation. Cybrid cells in the Ca^{2+} imaging experiment (Figure 16 and Figure 17B and C) exhibited a deregulation of cellular calcium upon TG perfusion after an initial stimulation with acetylcholine (AcCh), which was indicated by a significantly higher sustained cytoplasmic level of calcium above the basal level (Figure 17B and C). The deregulation of calcium was alleviated in the LHON cybrids by 100 µM minocycline and 3 µM CsA (Figure 17B). After the withdrawal of the excitatory stimulus, at 600 seconds of recording, the calcium fluorescent ratio values in minocycline (1.013 ± 0.017; n=5) and CsA (1.03 ± 0.005; n=5) treated groups significantly declined as compared to the AcCh/TG (1.069 ± 0.004; n=5) per se group. These differences in fluorescent ratios of the respective treatments were maintained through rest of the recordings. Two way ANOVA of the point in the graph after the withdrawal of thapsigargin revealed that there was a significant difference between treatment groups ($F(3,112)=39.01$, $p<0.001$). In the NT2 cell line however, no significant differences in the fluorescent values were observed and the insignificant calcium deregulation induced by AcCh/TG was not significantly alleviated by minocycline or CsA at any time point after the withdrawal of the stimulus (Figure 17B).

3.6 Mitochondrial membrane potential is conserved by minocycline

Cells stained with mitotracker green and TMRM are represented in Figure 18. A typical co-staining of the two fluorescent dye reveals a yellow color on overlapping. Results represented in Figure 19 shows that TG induced a significant decrease in the percentage of cells with active membrane potential in both cell lines (NT2 cells = $92.85 \pm 1.81\%$, $p<0.05$ and LHON cybrid = $68.54 \pm 1.6\%$, $p<0.01$). The degree of depolarization induced by thapsigargin in the two cell lines was also significantly different. The co-localization of TMRM and Mitotracker green, used as an indicator of functional mitochondria in proportion to the total population of mitochondria, was significantly increased in the 100 µM minocycline (88.29 ± 1.8 %, $p<0.01$) as well as 3 µM CsA (97.38 ± 0.39 %, $p<0.01$) treated groups in LHON cybrid cells (Figure 19B) ($F(2,111) = 89.25$ $p<0.01$). However, neither 100 µM minocycline (87.41 ± 2.14 %) nor 3 µM CsA
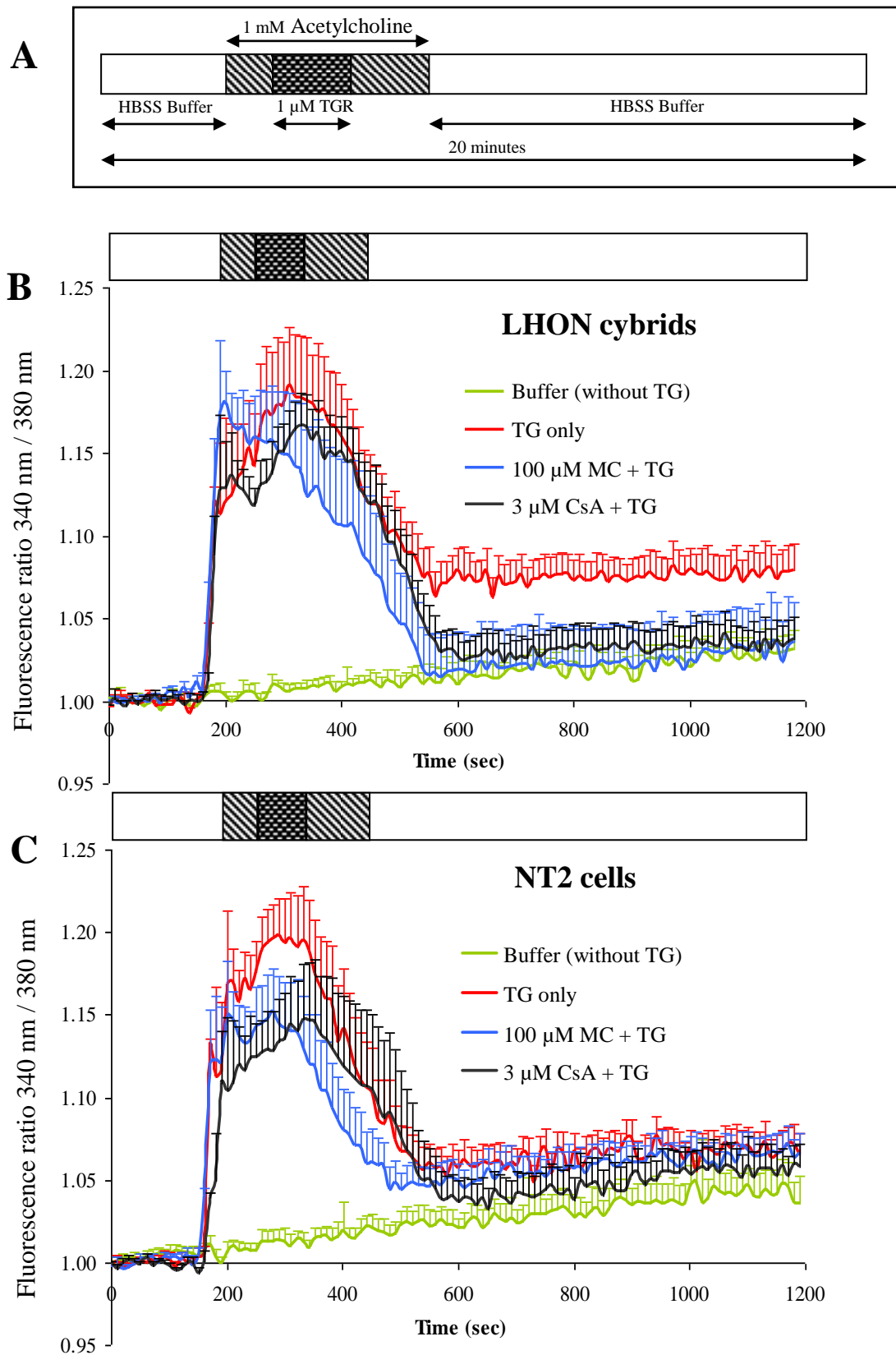
Figure 17: Graph of the calcium imaging experiments with different treatments. (A) A general layout of the experimental protocol, (B) live cell calcium imaging of LHON cybrid, and (C) live cell calcium imaging of NT2 cells. MC = minocycline.

Mitotracker Green	**TMRM**	**Overlap**

Control

TG

TG
+
Minocycline

TG
+
CsA
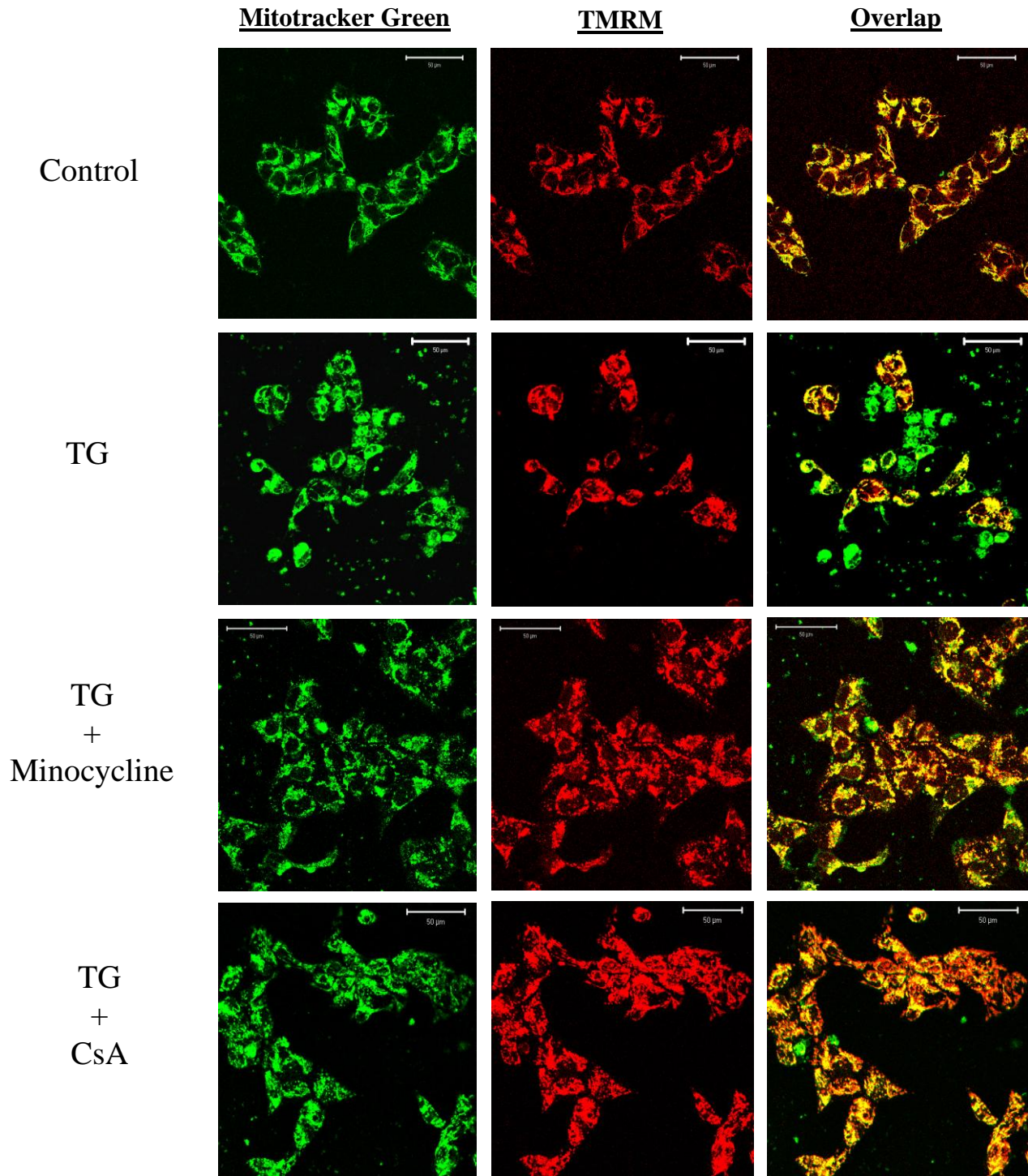
Figure 18: Mitochondrial membrane potential imaging by TMRM uptake in LHON cybrid cells. Cells were incubated with TG (1 µM) for 8 hours. Mitotracker green is taken up by all mitochondria, whereas TMRM stains only those that have intact membrane potential. The conservation of $\Delta\Psi_m$ by minocycline (100 µM) and CsA (3 µM) is observed when compared to cultures that were treated with TG alone. Scale bars are representative of 50 µm length.

$(90.56 \pm 2\%)$ was effective in conserving the mitochondrial membrane potential loss in the NT2 cells treated with TG (Figure 19A.) $(F_{(2,59)} = 1.253, p=0.29)$.
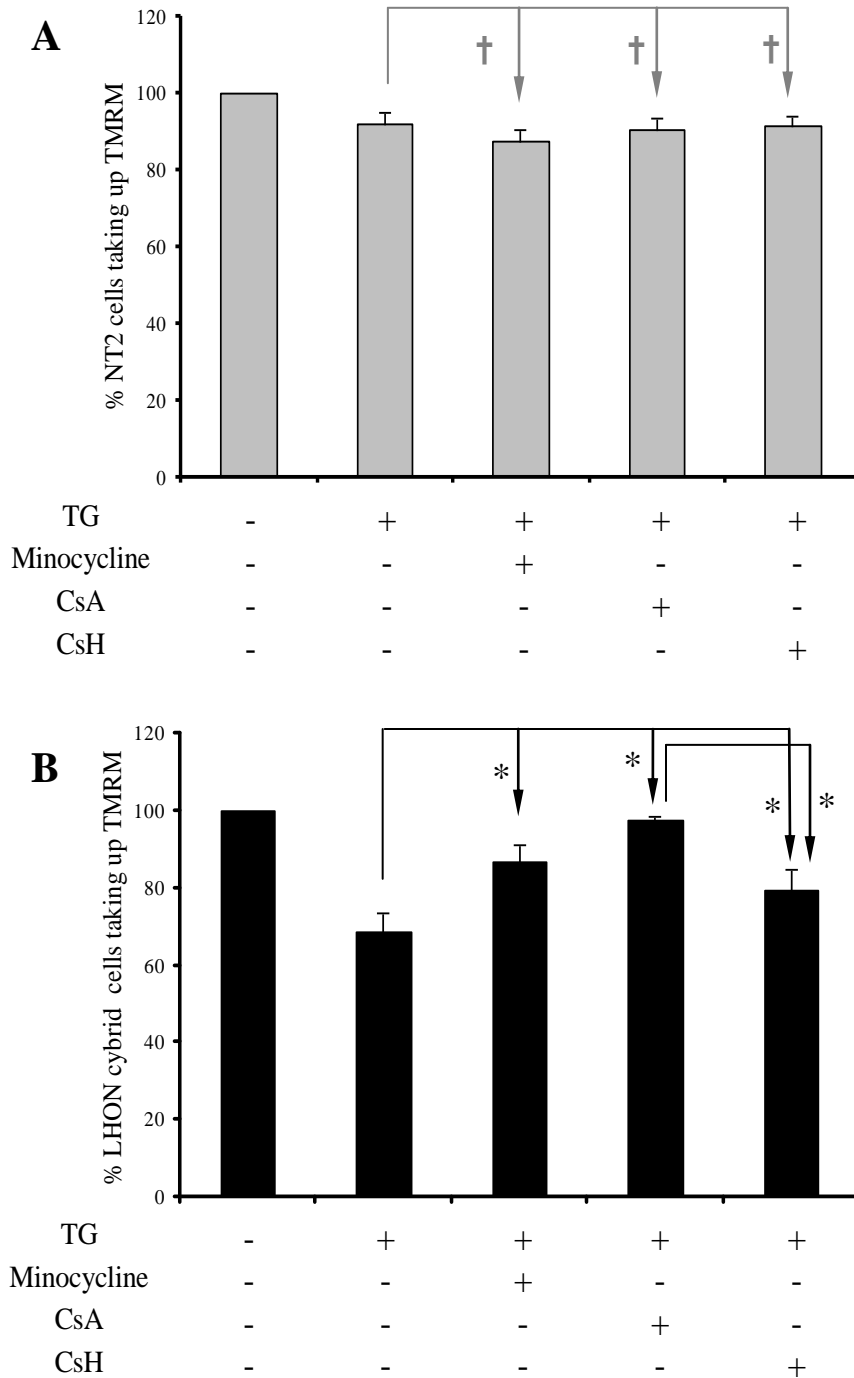
Figure 19: Percentage of cells with preserved mitochondrial membrane potential with minocycline, CsA and CSH treatments after TG incubation in LHON cybrid cells and NT2 (parental cell line) as indicated by the uptake of TMRM. (A) percentage of NT2 cells taking up TMRM, (B) percentage of LHON cybrids taking up TMRM. $*p<0.05$, $\dagger p>0.05$

The multidrug resistance (MDR) inhibition effect of CsA which can prevent the leakage of the dye from the cytoplasm and thereby give false positives were eliminated with the use of its congener cyclosporine H (CsH). CsH has a similar MDR inhibiting effect as that of CsA (Dietel et al., 1994: Foxwell et al., 1989) without the permeability transition blocking effect of CsA (Teplova et al., 2000; Woodfield et al., 1998). Experimentation with this congener could eliminate the MDR inhibiting activity of CsA in the uptake or retention of TMRM after thapsigargin insult. The results clearly showed the effects of CsH to be significantly lower than that of CsA suggesting that the increase of uptake shown by CsA was not dependant entirely upon the MDR inhibition property of the drug.

## 3.7 Active-caspase-3:procaspase-3 ratio is decreased by minocycline and cyclosporine A.

The effector caspase-3 activation is a downstream event in apoptosis. The opening of permeability transition and release of proapoptotic proteins like cytochrome c is responsible for the eventual activation of procaspase-3 to caspase-3 (active form). Western blots of LHON cybrid cells treated with TG showed an increase in the ratio of aC3/pC3 suggesting
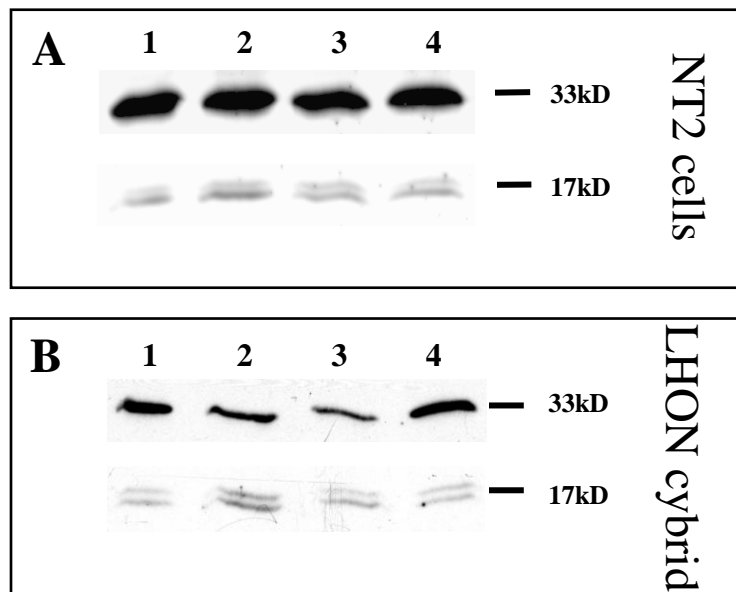
Figure 20: Representative Western blots of active-caspase 3 and procaspase 3 in NT2 (A) and LHON cybrid cells (B) following TG (1 µM) treatment for 8 hours. Cells were incubated with or without treatments (i.e. 100 µM minocycline or 3 µM CsA) in a serum free medium. Lane 1 = Control, 2 = incubation with 1 µM TG alone for 8 hrs, 3 = minocycline (100 µM) and, 4 = CsA (3 uM) treatment.

an activation of the downstream apoptotic event (Figure 20 and Figure 21). Quantification of the blots by densitometry exhibits a significant increase in the aC3/pC3 ratio in the LHON cybrids (2.82 ± 0.19; n=6) treated with TG comparing to NT2 cells (1.78 ± 0.18; n=5). Two-way ANOVA showed a significant effect of treatments on the aC3/pC3 ratio ($F_{(3,26)}=19.84$, $p<0.01$). A significant decrease in the ratio was seen in the LHON cybrid cells after minocycline (1.97 ± 0.16; n=7) or CsA (1.35 ± 0.23; n=7) treatments. In NT2 cells however, minocycline (1.34 ± 0.36; n=5), or CsA (1.1 ± 0.31; n=3), failed to significantly decrease the TG-induced rise of aC3/pC3 ratio.
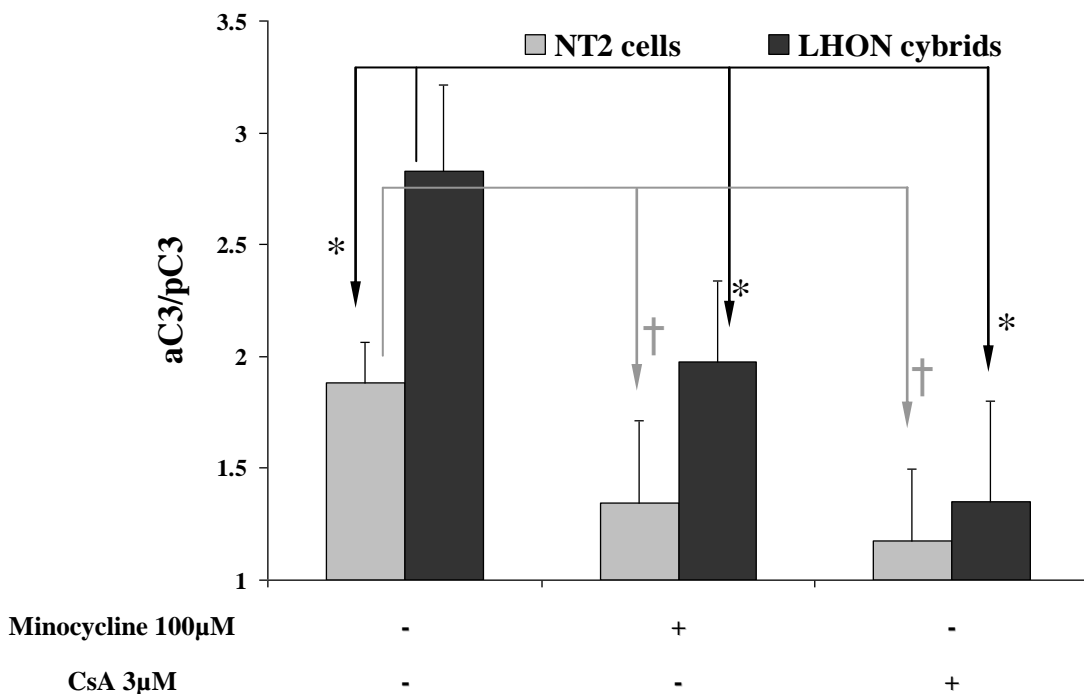
Figure 21: aC3/pC3 ratio of different groups is compared to the control (non thapsigargin treated: calculated as 1). Minocycline failed to significantly decrease the ratio in the NT2 cell lines but significantly reduced that in LHON cybrid cells. All bars represent groups treated with 1μM TG. Data are represented as arbitrary ratio units ± S.E.M. * $p<0.05$, † $p>0.05$.

3.8 Minocycline decreased the DFF fluorescence gain

Investigation of antioxidant properties of minocycline shows a significant dose dependent decrease in the DFF fluorescence by the drug. The basal level fluorescence in the LHON cybrids (35.94 ± 3.13) declined significantly with 100 μM (18.86 ± 4.18), 50 μM

(22.43 ± 1.38), and 25 μM (24.55 ± 2.87) but not with 10 μM (26.59 ± 4.1) minocycline, which suggests a dose dependent lowering in the oxidative stress level. The basal level fluorescence decline is comparable with the basal fluorescence observed in the NT2 cells (23.07 ± 1.6). Vitamin C as an antioxidant also brings down the basal oxidative level in the cybrid cells (19.35 ± 1.54, Figure 22). Subjecting the fluorescent intensities of the first 100 seconds of imaging to two way ANOVA between eight groups (NT2, LHON cybrids, LHON cybrids treated with four different minocycline concentrations, 3 μM CsA, and 100 μM vitamin C) reveals that the oxidative stress in the LHON cybrids was significantly lowered in both minocycline dose dependently (25 μM, 50 μM, and 100 μM) and vitamin C treatment at a concentration of 100 μM. This, however, is evident with the anti-apoptotic dose of CsA (36.59 ± 6.39) and the lowest dose of minocycline (10 μM) ($F_{(7,49)}$=4.924, $p<0.01$). A similar effect, as observed in the basal fluorescent intensities, was also seen with different concentrations of minocycline after H_2O_2 injection. An increase in fluorescent intensity was seen in the LHON cybrids in presence of H_2O_2 which significantly declined with minocycline and vitamin C treatment (Figure 23 and Figure 24). The live cell imaging shows that significant decrease in fluorescence intensities was observed with two of the higher but not the two lower doses of minocycline in comparison to the untreated group upon H_2O_2 injection in the culture (Figure 24 B).
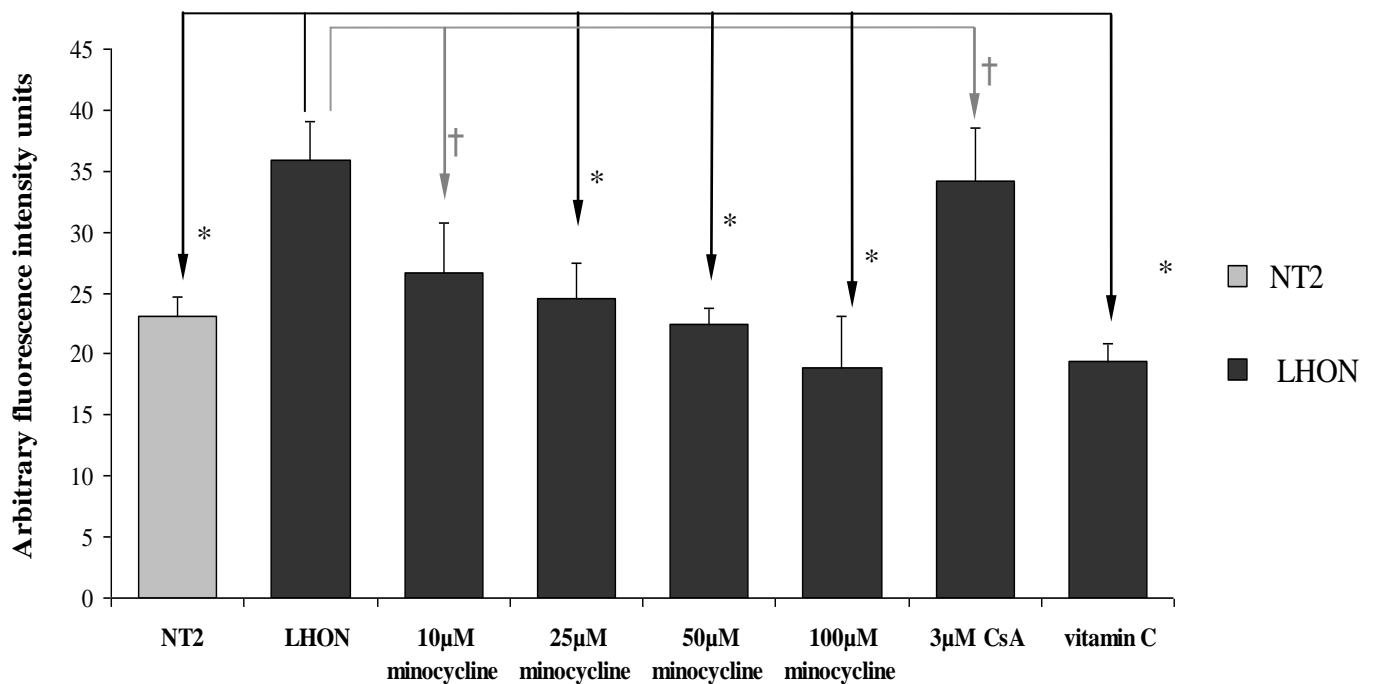
Figure 22: Average initial fluorescence intensities of first 100 seconds of imaging in different treatments. Significantly higher basal fluorescence intensity was observed in the LHON cybrid cells as compared to the parental NT2 cells, suggesting a higher level of oxidative stress in the cybrids.

Time (seconds)

0   255

Fluorescent intensities (pseudocolor scale)
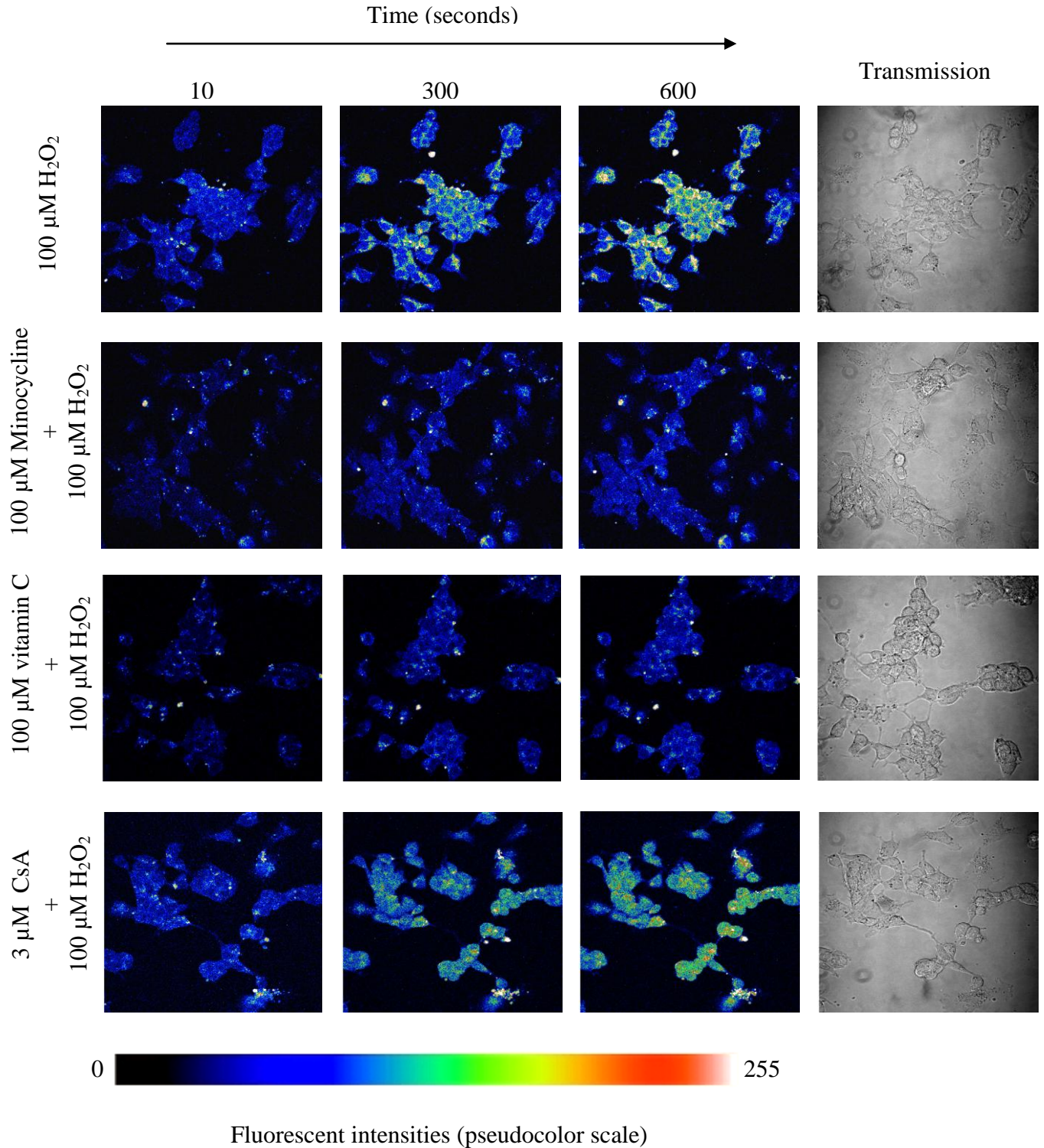
Figure 23: Representative DFF fluorescence live cell imaging of LHON cybrid cells. Confocal images of LHON cybrid cells stimulated with 100μM H_2O_2 with or without 100μM minocycline treatment. The images are converted to pseudo color corresponding to grey scale intensities of 0-255. Lower overall intensities are visible in the minocycline and vitamin c treated cultures.
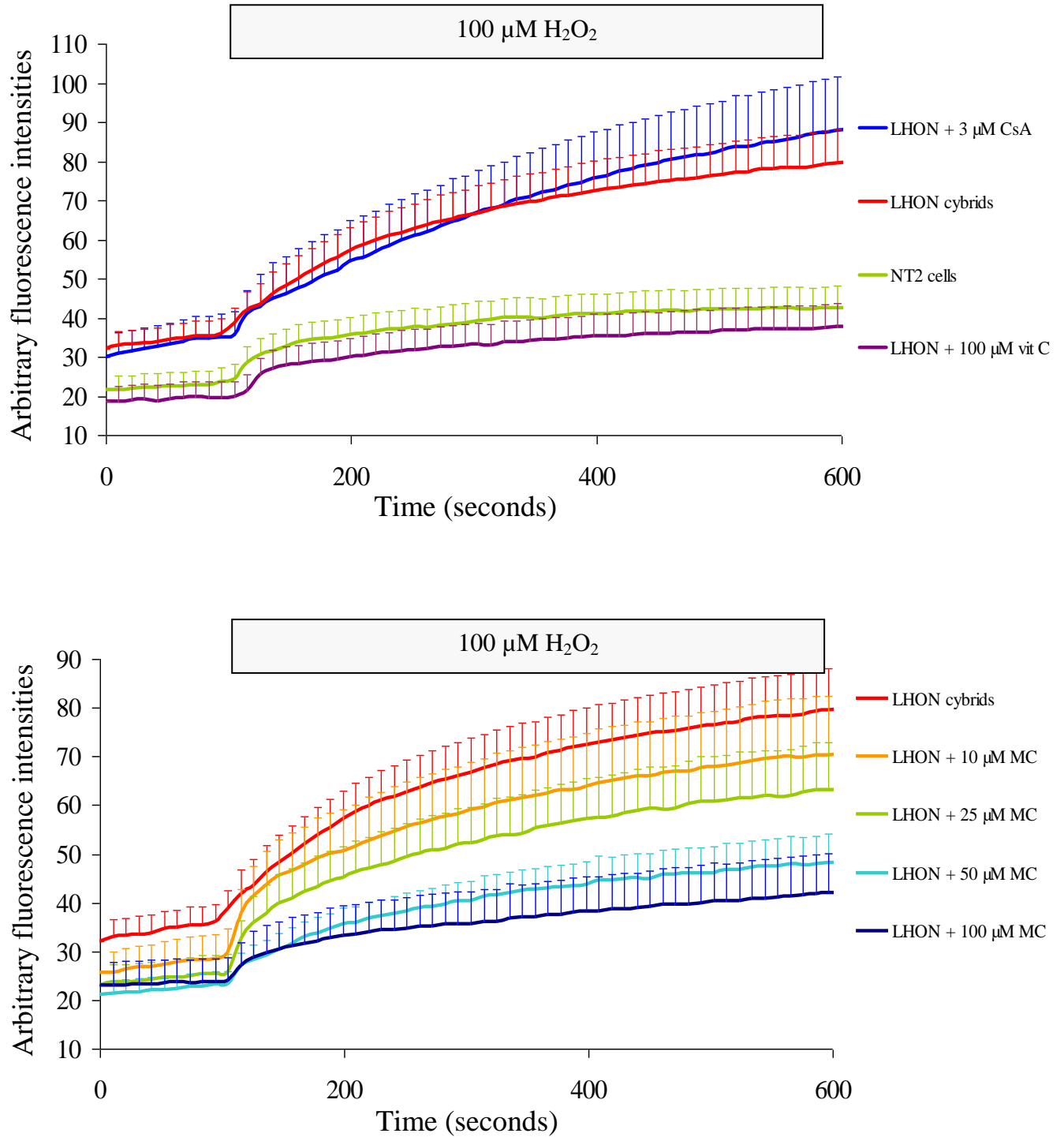
Figure 24: Comparative Graphs of DFF imaging with different treatments. (A) Comparison of DFF imaging fluorescence curve of NT2 cells with LHON cybrids stimulated with 100 μM H_2O_2 and the effect of CsA and vitamin C on the fluorescent intensities, (B) dose dependent decrease in DFF fluorescence by minocycline treatment in LHON cybrids. MC = minocycline; vit C = vitamin c.

4.   DISCUSSION

Mitochondria play a pivotal role in apoptotic signals. Other organelles like endoplasmic reticulum act in co-ordination with the mitochondria to initiate the apoptotic and cell death pathways. The endoplasmic reticulum appears to be the regulator of apoptosis as it is the main storehouse of cellular calcium and upon the release of these stores, calcium is quickly taken up by the juxtaposed mitochondria (Kim et al., 2006), which does not require the expenditure of ATP as it is driven by the mitochondrial membrane potential through the calcium uniporter in the IMM. An increase in the mitochondrial calcium results in an increase in the metabolic rate and production of free radicals, especially in conditions of respiratory chain defects. These combinations of scenarios thereby modulate the activity of the permeability transition (Smaili et al., 2000). Additionally, regulation of a steady state endoplasmic reticulum Ca^{2+} levels appears to be crucial checkpoint for Ca^{2+} dependent apoptosis. The involvement of deregulation of cytosolic and intra-mitochondrial calcium in neurodegeneration has been shown by researchers to constitute a major mitochondrial pathway to apoptosis through the opening of mtPTP (Jacquard, et al., 2006).

In this study a cybrid cell culture model of LHON disorder was used to investigate possible therapeutic interventions for the disease. For this purpose our model included for induction of cell death, the irreversible smooth endoplasmic reticular calcium ATPase (SERCA) inhibitor, TG (Lytton et al., 1991). An initial LD_{50} study of TG shows that 1 µM of the substance shows approximately 50% decrease in cell viability as presented by the outcome of MTT cell survival assays (Figure 10). TG, along with acetylcholine (in the calcium imaging experiments used to cause an initial release of calcium) inhibits the reuptake of calcium to the endoplasmic stores and, thus, augments mitochondrial calcium accumulation to mimic neuronal over-excitation (Hoek et al., 1997). Calcium being a positive effector of mitochondrial function, stimulates respiratory pathways and leads to generation of ROS (especially in case of respiratory defects which are also responsible for lower ATP generation) creating an ideal condition for mtPTP opening (Brookes et al., 2004). A possible therapeutic target would therefore be to lower oxidative stress along with blocking the mtPTP activity. We therefore investigated the effect of minocycline in the

aforementioned cell death model of LHON cybrids as it has been shown previously to possess both antioxidant and mtPTP blocking activity.

4.1 Increased cell viability in LHON model upon minocycline and cyclosporine A treatment

In the MTT cell viability assay minocycline demonstrated a significant protective effect in the LHON cybrid cells at a concentration of 100 μM and 125 μM in the model of TG induced cell death (Figure 11A). Further increase in the concentration apparently does not lead to a more pronounced protection against TG-induced cell death. On the contrary higher concentrations of minocycline (150 and 200 μM) were toxic to the cells. In the parental NT2 cells, however, TG had a much lower effect on decreasing the cell viability and minocycline was ineffective in providing protection at any tested concentration. In similar experiments, CsA was found to be comparatively effective in the cybrid cells at a concentration of 3 μM (Figure 11B). This was also observed in the calcium imaging experiments where the deregulation of calcium was likewise alleviated. In the NT2 cells however, none of the concentrations of CsA that were effective in the LHON cybrid cells, were found to be protective as demonstrated by the viability assay of TG treated cells (Figure 11 B). CsA being one of the most frequently and reliably used experimental inhibitor of mtPTP, these results suggest that the mtPTP may not play a significant role in decreasing the cell survival in the NT2 cells, whereas it does in the LHON cybrid cells.

The decrease percentage viability of NT2 cells by TG treatment can be attributed to the ER stress response and depletion of the Ca^{2+} stores (Kitamura et al., 2003, Yoshida et al., 2006). This would also be true for the LHON cybrid cells. On the other hand the MTT cell survival assay with the general caspase inhibitor z-VAD-FMK suggests that the cell death induced by TG is caspase independent i.e. non-apoptotic. DAPI staining however shows characteristic nuclear condensation, an absolute hallmark of apoptosis. As ATP levels are crucial for dictating the pathway of cell death (Leist et al., 1997), the ATP analysis also suggests cell death to be apoptotic in nature as the levels rise after an initial drop. Moreover, even under diminished conditions of ATP levels, a caspase independent form of cell death has been reported in other LHON cybrids (Zanna et al., 2005;

Zanna et al., 2003). For this type of apoptosis, the release of proapoptotic molecules from the intermembrane space was shown to elicit LHON cell death without the need of activating caspase-3. On the other hand, Western blot analysis reveals that the ratio of aC3/pC3 increases significantly more in the LHON cybrid cells than in the NT2 cells when treated with TG, and this ratio is decreased by CsA treatment in the LHON cybrids but not in NT2 cells indicating that the permeability transition is involved in LHON cybrids. Minocycline also significantly decreased the ratio in the cybrid cells but not in the NT2 cells. This is in concurrence with the results of the cell viability assay in which minocycline showed no significant protection at the observed concentration. On the other hand, however, the result of Western blotting and DAPI staining are also in conflict with the results of caspase inhibitor assay. The only evocative mechanism of cell death induced by TG in such a scenario, where the apoptosis is caspase independent, along with a suggestive involvement of mtPTP, would be the involvement of AIF (apoptosis inducing factor) or endonuclease G which are released from the mitochondria in apoptosis and translocates directly to the nucleus to cause nuclear condensation (van Loo et al., 2001; Daugas et al., 2000). This possibly also leaves other parallel mitochondrial apoptotic pathways intact, like the release of cytochrome c and eventually activation of downstream caspases, which explains the caspase-3 activation observed in western blotting. Immunocytochemistry of LHON cells treated with TG indeed revealed the involvement of permeability transition and the release of AIF from the mitochondria and its translocation to the cytoplasm and nucleus. There were few NT2 cells which also showed the AIF translocation which suggested that there is an extent of involvement of mtPTP in the parental cell line also, but, the population of such cells was small.

In the ATP measurements the decline of ATP level upon thapsigargin treatment in LHON cells (Figure 15) also points to mitochondrial damage by the calcium stimulus as a prerequisite of permeability transition and apoptosis (Brookes et al., 2004). Conservation of most ATP or even a re-establishment of normal levels of the same, after an initial decrease, may be necessary for the apoptosome to form, and thus for apoptosis to proceed (Figure 15). This phenomenon would not be necessary if the main pathway of apoptosis is through AIF release.

4.1.1 Inhibition of mtPTP as the target for neuroprotection in LHON

In a scenario where the reuptake of calcium back to the endoplasmic stores is inhibited by TG, mitochondria are expected to play the role of calcium buffering organelles that take up and thereby increase the matrix calcium concentration (Ichas and Mazat, 1998; Korge and Weiss, 1999). This leads to a stimulation of the respiratory chain and increases free radical generation (especially in the case of respiratory chain mutations) and eventually results in the opening of the mtPTP (Takeyama et al., 1993). Opening of the mtPTP leads to the release of mitochondrial calcium back into the cytosol. The normalization of calcium dynamics by mtPTP inhibition has previously been discussed (Bernardi and Petronilli, 1996, Rizzuto et al., 2000, Andrabi et al., 2004). In the performed live cell calcium imaging experiments minocycline had similar effects on cellular calcium dynamics as CsA in TG/AcCh-induced deregulation of calcium in the cybrid cells. There are previous reports showing that minocycline is able, like CsA, to inhibit the permeability transition in isolated brain and liver mitochondria (Zhu et al., 2002; Fernandez-Gomez et al., 2005a; Fuks et al., 2005). As seen in calcium imaging experiments the restoration of calcium dynamics suggests accordingly that in LHON cybrid cells minocycline is able to inhibit calcium overload-induced mtPTP formation significantly. In the parent cell line, applying the same set of experiments, neither minocycline nor CsA show any deviation of end calcium dynamics from TG per se group as observed in the LHON cybrid cells, which indicated that the mtPTP was not activated upon TG perfusion in the parental cell line. The increasing fluorescence ratio with buffer perfusion observed both in cybrid cells and the parental cell line is most likely due to leakage of the dye from the cell.

4.1.2 Mitochondrial membrane potential is conserved by minocycline

Mitochondrial $\Delta\Psi_m$ is the driving force of ATP production and the calcium buffering capacity of the mitochondria. The calcium is taken up by the mitochondria through a selective calcium uniporter and is accumulated at concentrations 100 times higher than in the cytosol. TMRM, a positively charged red fluorescent dye, is taken up by the mitochondria due to their negative $\Delta\Psi_m$ (Scaduto and Grotyohann, 1999). Upon opening of the mtPTP the $\Delta\Psi_m$ of mitochondria is lost (Blattner et al., 2001) and the dye is not taken

up. Mitotracker green, however, is taken up by mitochondria irrespective of their $\Delta\Psi_m$. The overlap of the two fluorescence images gives an idea of the proportion of cells that have intact mitochondrial $\Delta\Psi_m$. TG has been earlier shown to decrease the mitochondrial $\Delta\Psi_m$ (Yamazaki et al., 2006). The presented data also suggest that TG decreases the number of cells with preserved mitochondrial $\Delta\Psi_m$ and that in cybrid cells minocycline can conserve this loss of $\Delta\Psi_m$. The involvement of mtPTP in this set of experiments is confirmed by the conservation of mitochondrial $\Delta\Psi_m$ by CsA. These results are consistent with those obtained with live cell calcium imaging experiments and suggest that minocycline could act as anti-apoptotic agent by inhibiting the mtPTP. In NT2 cells even though the loss of mitochondrial $\Delta\Psi_m$ was significant in the TG treated group, minocycline and CsA did not significantly reverse the dissipation of $\Delta\Psi_m$, indicating that the mitochondrial $\Delta\Psi_m$ loss in the NT2 cells was CsA insensitive and therefore not due to mtPTP. The MDR inhibiting activity of CsA which might indicate false positives is eliminated by the use of its congener CsH, which possesses similar MDR inhibiting activity without mtPTP blocking effect, in similar set of experiments. If we consider the result obtained with CsH on TMRM uptake experiment as an indicative of similar MDR inhibiting activity of CsA and nullify the effect of former from that of latter, one could expect that the effect of CsA and minocycline on TMRM uptake would be comparable.

4.1.3 *LHON disorder could benefit from antioxidant property of minocycline*

As mentioned in the introduction, the symptoms of LHON disorder are influenced by age, gender and environmental factors which are commonly explained by a lacking capacity of the cell to encounter oxidative stress. With age the declining endogenous antioxidant pool and antioxidant enzyme activity of the cell can exaggerate the oxidative stress (Wei and Lee, 2002; Maher, 2005). In females the appearance of the LHON symptoms at a later age than in males can accordingly be explained by the presence of higher levels of oestrogen, an up-regulator of antioxidant genes (Vina et al., 2005). Smoking and alcohol consumption aggravate the oxidative load of the cell and consequently increase the relative risk of developing symptoms of LHON disorder (Tsao et al., 1999, Carelli et al., 2004a). The upregulation of cellular antioxidant systems has been shown to be a promising target to

rescue cells with LHON mutation (Qi et al., 2007a). In our study DFF imaging demonstrated a decrease in baseline fluorescence values with all except the lowest concentration of minocycline treatments similar to the decrease observed in vitamin c treatment. Additionally, the decrease was not observed with CsA as it lacks anti-oxidant properties. Induction of oxidative stress with H_2O_2 was dose dependently alleviated by minocycline as well as with 100μM vitamin C, but the same was not true for CsA treatment. These results support previous reports of antioxidant properties of minocycline (Kraus et al., 2005), which may contribute to its protective effect. Minocycline treatments reduced the basal fluorescent values and consequently the oxidative stress in LHON cybrids to a level where they are comparable to that observed in NT2 cells. The present findings suggest that minocycline, even at doses lower than 100 μM, can relieve the LHON cybrid cells of their inherent oxidative stress. The increase in cell viability seen in MTT assay was therefore not entirely dependent on the antioxidant property of the drug, but was also a consequence of mtPTP pore inhibition similar to that revealed in the performed experiments with CsA treatment, and in accordance with previous reports supporting minocycline to be an inhibitor of mtPTP (Zhu et al., 2002; Fernandez-Gomez et al., 2005a; Fuks et al., 2005).
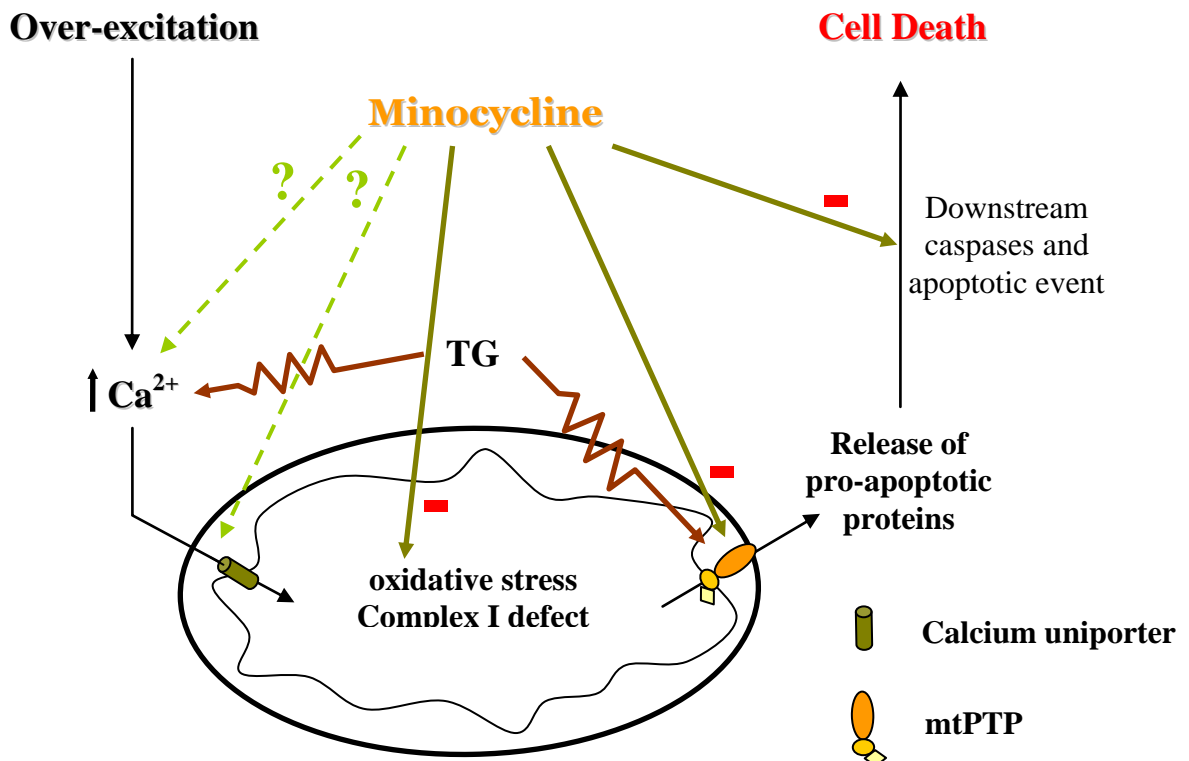
Figure 25: Possible targets of minocycline in preventing cell death of LHON cybrids.

4.2 Therapeutic strategies in LHON and minocycline

Advances in our understanding of the molecular genetic basis of LHON have revolutionized our ability to diagnose and prognosticate this disease. There are currently no clinical management protocols and specific therapeutic guidance for LHON and it presents formidable challenges to the design and conduction of clinical trials. The acutely symptomatic LHON patient with monocular vision loss provides a unique clinical situation of a limited duration in which to test an agent during a critical therapeutic window. Advances in neuroprotection, apoptosis, and neurodegenerative diseases may provide important clues for potential therapeutic agents for LHON. Antioxidants and agents that interfere with the critical steps of mitochondrial-dependent, oxidative stress-induced apoptosis are candidates for future LHON therapy (Johns and Colby 2002). A variety of neuroprotective agents, under active investigation in other diseases, may be useful in LHON therapy. Effective pharmacotherapy will complement the current management approach that has changed little in the 130 years since LHON was originally described. Recently a possibility of investigation of drugs in a mouse model of LHON has emerged which might accelerate drug development (Qi et al., 2007b). Therapies, targeting the function of the respiratory chain (ETC) and targeting ETC born ROS species are currently under discussion. At present, a clinical trial with the anti-oxidative ubiquinone-analogue idebenone is being performed in Great Britain and Germany, supervised by the Newcastle mitochondrial genetics group (Newcastle upon Tyne). In this trial, patients who developed recently LHON in one eye are experimentally treated with idebenone to rescue the second eye (second eye approach). Since individuals carrying a LHON mutation must not necessarily develop the disease, the risks of a general treatment of mutation carriers are considered to be too high. It is well known, especially from investigations of the large Brazilian pedigree (Sadun, et al., 2002; Sadun, et al., 2003; Sadun, et al., 2004), that even homoplasmic carriers must not necessarily develop the disease and that some additional risk factors, such as smoking exist. Precise ophthalmologic investigations may help to identify carriers prone to develop LHON in the near future. If some more data would have been collected in LHON models, the risk of applying the well established drug minocycline in such a "second eye approach" in humans may become tolerable.

Although 2.0 – 3.0 µM CsA reversed partially the TG induced toxicity the long term usage of such concentrations *in vivo* is certainly not applicable to human LHON disease. Blood concentrations in the target levels of 180 - 300 ng/ml (0.15 - 0.25 µM), occurring if CsA is used as an immunosuppressive drug, are known to cause several side effects in a considerable percentage of patients. Besides increased arterial blood pressure, also several neurological complications have been described, such as tremor (in up to 40 % of cases), mild encephalophathy (in up to 30 %), seizures (1.5 – 6 %), dysarthria, cerebellar ataxia and peripheral neuropathy (Gijtenbeek, et al., 1999). Thus *in vivo* the toxic side effects seem to exceed the desired protective effects, measurable in the cybrid system. In contrast minocycline has a high safety profile and possess antioxidant properties, as demonstrated by the live cell DFF-imaging the LHON cybrid model. On the other hand, the achieved serum peak concentrations of minocycline in humans is about 5 - 6 µg/ml (around 12 µM) after 200 mg intravenous application. It remains uncertain, whether sufficient tissue concentrations can be reached. In case of LHON, the blood brain barrier has to be taken into account, which probably allows only a fraction of this concentration to reach the retinal ganglion cell layer and the optic nerve. However, recently it has been shown that in blood-brain barrier transport studies in mice after intra-peritoneal injection of 90 mg minocycline / kg and determined plasma concentrations of minocycline in the range of 40 – 60 µg/ml (around 80 – 120 µM) and corresponding brain/plasma ratio around 0,08 (corresponding to about 6 – 9 µM uptake into the CNS) (Milane, 2007). Similar results (2.8 µg/ml; approx. 6 µM) have been reported for cerebrospinal fluid from rats (Fagan, et al., 2004). After oral administration (120 mg/kg) in mice after 8 hours midbrain minocycline levels of 0.32 µg/g were described (Du, et al., 2001). To the present knowledge, no data are currently available concerning minocycline concentrations in retina or optic nerve. Theoretically, a direct application of minocycline into the vitreous maybe taken into account, as it is already performed nowadays with e.g. anti-inflammatory drugs in some cases. However, this possibility seems to be rather unrealistic, since even the acute phase of LHON must be viewed only as a manifestation of a basically chronic retinal disease, which would require a long term neuroprotective medication. The drug can be delivered efficiently only via oral or other systemic routes. The surprisingly small window of effective concentrations found in current experiments (100 –125 µM) is in contrast to the broader therapeutic window observed during antibiotic therapy *in vivo*. This difference may just reflect the ineffective uptake of minocycline by the cybrid cells or possibly a higher rate of metabolic breakdown

in which case the effective *in vivo* concentrations can predictably be lower. However, the higher tolerability and effectiveness exhibited by minocycline in the cybrid cells will most likely not be manifested in higher animal studies. Further studies are necessary to determine the local concentration needed in the retina and around the optic nerve and to find out a relevant minocycline concentration in relation to a route of drug administration to attain neuroprotection *in-vivo*. On the way to that point, it would be highly interesting, to test the potential benefit of minocycline in a mouse LHON model, which was recently developed by the group of John Guy who showed for the first time that a transfection of mouse retina with viral vectors, allotopically expressing a mutant human ND4 subunit did develop elevated ROS production, optical nerve head swelling, apoptosis and progressive loss of retinal ganglion cells (Qi et al., 2007b). These effects did not occur in mice transfected with wild type human ND4. This was the first true genetic animal model of LHON, which should be suitable *in vivo* pharmaceutical drug testing model, prior to a "second eye approach" in humans.

The lack of sufficient uptake into the CNS and a probably narrow range of useful concentrations, as shown in this study to be higher than that which is clinically achievable in the retinal ganglion cell layer, might however, limit the usefulness of minocycline in LHON therapy. Also the controversially discussed effects of minocycline in various models of neurodegeneration and neuroprotection restrict a conclusive assumption of its usefulness. Furthermore, it is difficult to directly correlate the protective effects of minocycline in our relatively simple model of LHON to the RGC layer, where we cannot yet completely comprehend the complexities of the *in-vivo* environment and the nature of possible interactions of the ganglions with their surroundings. Nevertheless, we conclude that the protective effect shown by minocycline in the present experiments on LHON cybrid cells, along with its well-established clinical use, makes it an interesting drug for further investigations in therapy of LHON disease, possibly as a next step, in a mutant ND4 transgenic mouse like that described by Qi et al. (Qi et al., 2007b).

5.   SUMMARY

Leber's Hereditary Optic Neuropathy (LHON) is a retinal ganglionic neurodegenerative disorder caused by a maternally inherited mitochondrial DNA point mutation. The dysfunction of complex I of the respiratory chain, affected by the mutation, results in an increased production of reactive oxygen species and a decreased synthesis of ATP. This biochemical scenario can lead to an imbalance in the production and demand of energy required for cell survival. In such a state the cell may die by apoptosis, which in LHON disorder is most prominently apparent as optic nerve degeneration. Cybrid cells are the most frequently used model for this disease as the optic nerve of a LHON patient is not accessible until the death of the patient and by which time the degeneration is to its full extent.

The aim of this study was the establishment of a cell-mediated LHON-model for evaluation of antioxidants and neuroprotective drugs and to discover the involvement of the mitochondrial permeability transition pore (mtPTP) in development of the disorder. Using cybrid cells harbouring the mitochondrial 11778 LHON point mutation, the efficacy of the promising neuroprotective tetracycline derivative minocycline was investigated. The drug increased the cell viability of LHON cybrids in the MTT assay after addition of the apoptotic stimulus, thapsigargin (TG). In contrast, this pattern of protection was not evident in the parental control cell line (NT2). A comparable protection to minocycline was observed by treatment with cyclosporine A (CsA), a well known blocker of the mtPTP. Furthermore, a general caspase inhibitor (z-VAD-FMK) did not prevent the thapsigargin-induced cell death in either of the cell lines. Whereas, staining of the nuclei with DAPI showed nuclear condensation and apoptotic morphology of the cell. In support of this, immunocytochemistry revealed the release of the apoptosis-inducing factor (AIF) from the mitochondria and translocation to the nucleus, suggesting an mtPTP-induced caspase independent apoptosis. Ratiometric Ca^{2+} imaging reveals that acetylcholine/TG triggered elevation of the cytosolic calcium concentration is alleviated by both minocycline and CsA, also suggesting an involvement of permeability transition. In addition the mitochondrial membrane potential ($\Delta\Psi_m$) of LHON cybrid cells, as evaluated by the uptake of TMRM, was significantly conserved with both minocycline and CsA treatments. Western blots

showed a decrease in the ratio of active-caspase-3 to procaspase-3 proteins in the minocycline and CsA treated groups of cybrid cells after TG-induced cell death, which suggests the regulation of downstream apoptotic events. This is in contradiction to the obtained results in the MTT assay using z-VAD-FMK, which indicates that the TG-triggered cell death is a non-caspase-dependent process. The release of pro-apoptotic factors (e.g. AIF) from the mitochondria is the proposed mechanism of cell death. But parallel pathways, causing activation of caspases, are also possibly active. Blockade of the mtPTP opening by CsA and minocycline prevents death of the LHON cybrids. Additionally, minocycline dose dependently decreased the oxidative stress in LHON cells, supporting the effective anti-oxidant property of this tetracycline.

In conclusion, the opening of the mtPTP is involved in the onset of LHON and minocycline provides beneficial effects, beside its antioxidant property, through inhibition of mtPTP. Further investigation into the effect of minocycline, possibly in an *in vivo* model of the disease, such as a LHON ND4 mutant mouse, would be necessary to prove its protective mechanisms on the retinal ganglionic cell layer and the optic nerve.

6. ZUSAMMENFASSUNG

Die Lebersche hereditäre Optikusneuropathie (LHON) ist eine neurodegenerative Erkrankung des Sehnervs, die von der Mutter weitervererbt und durch Punktmutationen der mitochondrialen DNA verursacht wird. Die Fehlfunktion des betroffenen Komplexes I der Atmungskette führt zu einer erhöhten Produktion reaktiver Sauerstoffspezies und einer Abnahme der ATP-Synthese. Diese Situation kann ein Ungleichgewicht zwischen der Herstellung und der zum Überleben der Zelle benötigten Menge an Energie zu Folge haben. Unter solchen Bedingungen könnte die Zelle durch Apoptose sterben, was bei LHON als Degeneration des Sehnervs offenkundig wird. Cybrid-Zellen sind das am häufigsten benutzte Modell für diese Erkrankung, da der Sehnerv von LHON-Patienten erst nach dem Tod zugänglich und zu diesem Zeitpunkt die Degeneration meist in vollem Umfang ausgeprägt ist.

Ziel der Untersuchungen war die Etablierung eines zellulären Schädigungsmodells für LHON, um einerseits die Wirkung von Antioxidantien und Neuroprotektiva zu beurteilen und andererseits die Beteiligung der mitochondrialen Permeabilitätstransitionspore (mtPTP) bei der Ausprägung der Erkrankung zu untersuchen. Unter Verwendung von Cybrid-Zellen mit einer mitochondrialen LHON-Mutation an Position 11778 wurde die Wirksamkeit des vielversprechenden neuroprotektiven Tetracyclin-Derivats Minocyclin untersucht. Das Medikament erhöhte die Lebensfähigkeit der LHON-Cybrid-Zellen in MTT-Analysen nach Applikation des Apoptose auslösenden Stimulus Thapsigargin (TG). In der als Kontrolle verwendeten Ausgangszelllinie NT2 war im Gegensatz dazu diese Art des Schutzes nicht nachweisbar. Eine zu Minocyclin vergleichbare Protektion wurde nach Behandlung mit Cyclosporin A (CsA), einem bekannten Blocker der mtPTP, beobachtet. Der Einsatz eines allgemeinen Caspase-Inhibitors (z-VAD-FMK) konnte den durch TG induzierten Zelltod in keiner der beiden Zelllinien verhindern. Hingegen waren die Kondensation des Chromatins, detektiert mittels DAPI-Färbung, und die apoptotische Morphologie der Zellen erkennbar. Weiterhin konnte immunhistochemisch die Freisetzung des Apoptose induzierenden Faktors (AIF) aus den Mitochondrien und dessen Translokation in den Zellkern nachgewiesen werden, was auf mtPTP induzierte und Caspasen unabhängige Apoptose hinweist. Ratiometrische Messungen des intrazellulären Ca^{2+} ergaben, dass die durch

Acetylcholin/TG ausgelöste Erhöhung der cytosolischen Ca^{2+}-Konzentration durch Minocyclin und CsA abgeschwächt wird, was ebenfalls für eine Beteiligung der mtPTP spricht. Zusätzlich war das mitochondriale Membranpotential ($\Delta\Psi_m$) der LHON-Cybrid-Zellen, ermittelt durch die Aufnahme von TMRM, signifikant besser konserviert nach einer Behandlung mit Minocycline und CsA. Western blot-Analysen zeigten eine Abnahme des Verhältnisses von aktivierter Caspase 3 zu Procaspase 3 in den mit Minocyclin und CsA behandelten Gruppen nach TG-induziertem Zelltod, was auf die Regulation nachgeschalteter apoptotischer Ereignisse hinweist. Dies steht jedoch im Widerspruch zu den unter Verwendung von z-VAD-FMK erhaltenen Ergebnissen in den MTT-Experimenten, welche auf einen Caspase unabhängigen Prozess hindeuten. Die Abgabe pro-apoptotischer Faktoren (z.B. AIF) von Mitochondrien und die Aktivierung von Caspasen stellen die Ursache für den beobachteten Zelltod dar. Eine Blockade der Öffnung der mtPTP durch CsA und Minocyclin kann den Untergang der LHON-Cybride verhindern. Zusätzlich verringerte Minocyclin konzentrationsabhängig den oxidativen Stress in LHON-Zellen, was die guten antioxidativen Eigenschaften dieses Tetracyclins bestätigt.

Schlussfolgernd ist festzustellen, dass ein Öffnen der mtPTP an der Pathogenesse der LHON beteiligt ist und Minocyclin, neben seiner Eigenschaft als Antioxidant, vorteilhafte Effekte durch die Hemmung der mtPTP besitzt. Weitere Untersuchungen zu den Auswirkungen von Minocyclin in *in vivo* Modellen dieser Erkrankung (z.B. an Mäusen mit ND4-Mutation) sind erforderlich, um den schützenden Mechanismus an retinalen Ganglienzellen und Sehnerv zu beweisen.

7.   ABBREVIATIONS

$\Delta\Psi_m$	mitochondrial membrane potential
aC3/pC3	active-caspase 3/pro-caspase 3
AIF	apoptosis inducing factor
ALS	amyotrophic lateral sclerosis
ANT	adenosine nucleoside translocase
ATP	adenosine triphosphate
BCA	bicinchoninic acid
BSA	bovine serum albumin
CsA	cyclosporin A
CsH	cyclosporin H
CoQ	coenzyme Q
Cyc	cytochrome c
CyP D	cyclophilin D
DFF	difluorofluorescein
DIABLO	direct inhibitor of apoptosis protein binding protein with low pI
DMEM	Dulbecco modified Eagle's medium
EAAT	excitatory amino acid transporter
ER	Endoplasmic reticulum
ETC	electron transport chain
FAD	flavin adenine dinucleotide
FCS	fetal Calf Serum
H_2O_2	hydrogen peroxide
LHON	Leber's hereditary optic neuropathy
MDR	multidrug resistance pump
mtPTP	mitochondrial permeability transition pore
mtDNA	mitochondrial DNA
MTT	methylthiazolyldiphenyl-tetrazolium bromide
NADP	nicotinamide adenine dinucleotide phosphate
OMM	outer mitochondrial membrane

PBS	phosphate buffer saline
PDL	poly-D-lysine
PT	permeability transition
rcf	relative centrifugal force
RGC	retinal ganglionic cells
ROI	region of interest
ROS	reactive oxygen species
SMAC	second mitochondria-derived activator of caspases
SR	sarcoplasmic reticulum
TG	thapsigargin
TMRM	tetramethyl rhodamine methyl ester
UP	calcium uniporter
VDAC	voltage dependent anionic channel

8.   REFERENCES

Amin, A. R., Attur, M. G., Thakker, G. D., Patel, P. D., Vyas, P. R., Patel, R. N., Patel, I. R. and Abramson, S. B., 1996. A novel mechanism of action of tetracyclines: effects on nitric oxide synthases. Proc Natl Acad Sci U S A. 93, 14014-14019.

Andrabi, S. A., Sayeed, I., Siemen, D., Wolf, G. and Horn, T. F., 2004. Direct inhibition of the mitochondrial permeability transition pore: a possible mechanism responsible for anti-apoptotic effects of melatonin. Faseb J. 18, 869-871.

Baracca, A., Solaini, G., Sgarbi, G., Lenaz, G., Baruzzi, A., Schapira, A. H., Martinuzzi, A. and Carelli, V., 2005. Severe impairment of complex I-driven adenosine triphosphate synthesis in leber hereditary optic neuropathy cybrids. Arch Neurol. 62, 730-736.

Basso, E., Fante, L., Fowlkes, J., Petronilli, V., Forte, M. A. and Bernardi, P., 2005. Properties of the permeability transition pore in mitochondria devoid of Cyclophilin D. J Biol Chem. 280, 18558-18561.

Battisti, C., Formichi, P., Cardaioli, E., Bianchi, S., Mangiavacchi, P., Tripodi, S. A., Tosi, P. and Federico, A., 2004. Cell response to oxidative stress induced apoptosis in patients with Leber's hereditary optic neuropathy. J Neurol Neurosurg Psychiatry. 75, 1731-1736.

Beattie, M. S., 2004. Inflammation and apoptosis: linked therapeutic targets in spinal cord injury. Trends Mol Med. 10, 580-583.

Beretta, S., Mattavelli, L., Sala, G., Tremolizzo, L., Schapira, A. H., Martinuzzi, A., Carelli, V. and Ferrarese, C., 2004. Leber hereditary optic neuropathy mtDNA mutations disrupt glutamate transport in cybrid cell lines. Brain. 127, 2183-2192.

Bernardi, P., Vassanelli, S., Veronese, P., Colonna, R., Szabo, I. and Zoratti, M., 1992. Modulation of the mitochondrial permeability transition pore. Effect of protons and divalent cations. J Biol Chem. 267, 2934-2939.

Bernardi, P. and Petronilli, V., 1996. The permeability transition pore as a mitochondrial calcium release channel: a critical appraisal. J Bioenerg Biomembr. 28, 131-138.

Blattner, J. R., He, L. and Lemasters, J. J., 2001. Screening assays for the mitochondrial permeability transition using a fluorescence multiwell plate reader. Anal Biochem. 295, 220-226.

Bohr, V. A. and Anson, R. M., 1999. Mitochondrial DNA repair pathways. J Bioenerg Biomembr. 31, 391-398.

Bonelli, R. M., Hodl, A. K., Hofmann, P. and Kapfhammer, H. P., 2004. Neuroprotection in Huntington's disease: a 2-year study on minocycline. Int Clin Psychopharmacol. 19, 337-342.

Broekemeier, K. M., Dempsey, M. E. and Pfeiffer, D. R., 1989. Cyclosporin A is a potent inhibitor of the inner membrane permeability transition in liver mitochondria. J Biol Chem. 264, 7826-7830.

Brookes, P. S., Yoon, Y., Robotham, J. L., Anders, M. W. and Sheu, S. S., 2004. Calcium, ATP, and ROS: a mitochondrial love-hate triangle. Am J Physiol Cell Physiol. 287, C817-833.

Brown, M. D., Voljavec, A. S., Lott, M. T., MacDonald, I. and Wallace, D. C., 1992. Leber's hereditary optic neuropathy: a model for mitochondrial neurodegenerative diseases. Faseb J. 6, 2791-2799.

Brown, M. D., 1999. The enigmatic relationship between mitochondrial dysfunction and Leber's hereditary optic neuropathy. J Neurol Sci. 165, 1-5.

Carelli, V., Ghelli, A., Ratta, M., Bacchilega, E., Sangiorgi, S., Mancini, R., Leuzzi, V., Cortelli, P., Montagna, P., Lugaresi, E. and Degli Esposti, M., 1997. Leber's hereditary optic neuropathy: biochemical effect of 11778/ND4 and 3460/ND1 mutations and correlation with the mitochondrial genotype. Neurology. 48, 1623-1632.

Carelli, V., Ghelli, A., Bucchi, L., Montagna, P., De Negri, A., Leuzzi, V., Carducci, C., Lenaz, G., Lugaresi, E. and Degli Esposti, M., 1999. Biochemical features of mtDNA 14484 (ND6/M64V) point mutation associated with Leber's hereditary optic neuropathy. Ann Neurol. 45, 320-328.

Carelli, V., Ross-Cisneros, F. N. and Sadun, A. A., 2004. Mitochondrial dysfunction as a cause of optic neuropathies. Prog Retin Eye Res. 23, 53-89.

Carelli, V., Rugolo, M., Sgarbi, G., Ghelli, A., Zanna, C., Baracca, A., Lenaz, G., Napoli, E., Martinuzzi, A. and Solaini, G., 2004. Bioenergetics shapes cellular death pathways in Leber's hereditary optic neuropathy: a model of mitochondrial neurodegeneration. Biochim Biophys Acta. 1658, 172-179.

Chen, M., Ona, V. O., Li, M., Ferrante, R. J., Fink, K. B., Zhu, S., Bian, J., Guo, L., Farrell, L. A., Hersch, S. M., Hobbs, W., Vonsattel, J. P., Cha, J. H. and Friedlander, R. M.,

2000. Minocycline inhibits caspase-1 and caspase-3 expression and delays mortality in a transgenic mouse model of Huntington disease. Nat Med. 6, 797-801.

Chu, L. S., Fang, S. H., Zhou, Y., Yu, G. L., Wang, M. L., Zhang, W. P. and Wei, E. Q., 2007. Minocycline inhibits 5-lipoxygenase activation and brain inflammation after focal cerebral ischemia in rats. Acta Pharmacol Sin. 28, 763-772.

Crompton, M., 1999. The mitochondrial permeability transition pore and its role in cell death. Biochem J. 341 (Pt 2), 233-249.

Danielson, S. R., Wong, A., Carelli, V., Martinuzzi, A., Schapira, A. H. and Cortopassi, G. A., 2002. Cells bearing mutations causing Leber's hereditary optic neuropathy are sensitized to Fas-Induced apoptosis. J Biol Chem. 277, 5810-5815.

Daugas, E., Susin, S. A., Zamzami, N., Ferri, K. F., Irinopoulou, T., Larochette, N., Prevost, M. C., Leber, B., Andrews, D., Penninger, J. and Kroemer, G., 2000. Mitochondrio-nuclear translocation of AIF in apoptosis and necrosis. Faseb J. 14, 729-739.

Denton, R. M. and McCormack, J. G., 1986. The calcium sensitive dehydrogenases of vertebrate mitochondria. Cell Calcium. 7, 377-386.

Desjardins, P., de Muys, J. M. and Morais, R., 1986. An established avian fibroblast cell line without mitochondrial DNA. Somat Cell Mol Genet. 12, 133-139.

Dietel, M., Herzig, I., Reymann, A., Brandt, I., Schaefer, B., Bunge, A., Heidebrecht, H. J. and Seidel, A., 1994. Secondary combined resistance to the multidrug-resistance-reversing activity of cyclosporin A in the cell line F4-6RADR-CsA. J Cancer Res Clin Oncol. 120, 263-271.

DiMauro, S., 2004. Mitochondrial diseases. Biochim Biophys Acta. 1658, 80-88.

Dimauro, S. and Davidzon, G., 2005. Mitochondrial DNA and disease. Ann Med. 37, 222-232.

Du, Y., Ma, Z., Lin, S., Dodel, R. C., Gao, F., Bales, K. R., Triarhou, L. C., Chernet, E., Perry, K. W., Nelson, D. L., Luecke, S., Phebus, L. A., Bymaster, F. P. and Paul, S. M., 2001. Minocycline prevents nigrostriatal dopaminergic neurodegeneration in the MPTP model of Parkinson's disease. Proc Natl Acad Sci U S A. 98, 14669-14674. Epub 12001 Nov 14627.

Elewa, H. F., Hilali, H., Hess, D. C., Machado, L. S. and Fagan, S. C., 2006. Minocycline for short-term neuroprotection. Pharmacotherapy. 26, 515-521.

Erickson, R. P., 1972. Leber's optic atrophy, a possible example of maternal inheritance. Am J Hum Genet. 24, 348-349.

Fagan, S. C., Edwards, D. J., Borlongan, C. V., Xu, L., Arora, A., Feuerstein, G., Hess, D. C., 2004. Optimal delivery of minocycline to the brain: implication for human studies of acute neuroprotection. Exp Neurol. 186(2), 248-51.

Fehlings, M. G. and Baptiste, D. C., 2005. Current status of clinical trials for acute spinal cord injury. Injury. 36 Suppl 2, B113-122.

Fernandez-Gomez, F. J., Galindo, M. F., Gomez-Lazaro, M., Gonzalez-Garcia, C., Cena, V., Aguirre, N. and Jordan, J., 2005. Involvement of mitochondrial potential and calcium buffering capacity in minocycline cytoprotective actions. Neuroscience. 133, 959-967.

Fernandez-Gomez, F. J., Gomez-Lazaro, M., Pastor, D., Calvo, S., Aguirre, N., Galindo, M. F. and Jordan, J., 2005. Minocycline fails to protect cerebellar granular cell cultures against malonate-induced cell death. Neurobiol Dis. 20, 384-391.

Festoff, B. W., Ameenuddin, S., Arnold, P. M., Wong, A., Santacruz, K. S. and Citron, B. A., 2006. Minocycline neuroprotects, reduces microgliosis, and inhibits caspase protease expression early after spinal cord injury. J Neurochem. 97, 1314-1326.

Floreani, M., Napoli, E., Martinuzzi, A., Pantano, G., De Riva, V., Trevisan, R., Bisetto, E., Valente, L., Carelli, V. and Dabbeni-Sala, F., 2005. Antioxidant defences in cybrids harboring mtDNA mutations associated with Leber's hereditary optic neuropathy. Febs J. 272, 1124-1135.

Foxwell, B. M., Mackie, A., Ling, V. and Ryffel, B., 1989. Identification of the multidrug resistance-related P-glycoprotein as a cyclosporine binding protein. Mol Pharmacol. 36, 543-546.

Fuks, B., Talaga, P., Huart, C., Henichart, J. P., Bertrand, K., Grimee, R. and Lorent, G., 2005. In vitro properties of 5-(benzylsulfonyl)-4-bromo-2-methyl-3(2H)-pyridazinone: a novel permeability transition pore inhibitor. Eur J Pharmacol. 519, 24-30.

Gabler, W. L. and Creamer, H. R., 1991. Suppression of human neutrophil functions by tetracyclines. J Periodontal Res. 26, 52-58.

Ghelli, A., Zanna, C., Porcelli, A. M., Schapira, A. H., Martinuzzi, A., Carelli, V. and Rugolo, M., 2003. Leber's hereditary optic neuropathy (LHON) pathogenic mutations induce mitochondrial-dependent apoptotic death in transmitochondrial cells incubated with galactose medium. J Biol Chem. 278, 4145-4150.

Gijtenbeek, J. M., van den Bent, M. J. and Vecht, C. J., 1999. Cyclosporine neurotoxicity: a

review. J Neurol. 246, 339-346.

Gincel, D., Zaid, H. and Shoshan-Barmatz, V., 2001. Calcium binding and translocation by
the voltage-dependent anion channel: a possible regulatory mechanism in
mitochondrial function. Biochem J. 358, 147-155.

Gordon, P. H., Moore, D. H., Miller, R. G., Florence, J. M., Verheijde, J. L., Doorish, C.,
Hilton, J. F., Spitalny, G. M., Macarthur, R. B., Mitsumoto, H., Neville, H. E.,
Boylan, K., Mozaffar, T., Belsh, J. M., Ravits, J., Bedlack, R. S., Graves, M. C.,
McCluskey, L. F., Barohn, R. J. and Tandan, R., 2007. Efficacy of minocycline in
patients with amyotrophic lateral sclerosis: a phase III randomised trial. Lancet
Neurol. 6, 1045-1053.

Green, D. R. and Kroemer, G., 2004. The pathophysiology of mitochondrial cell death.
Science. 305, 626-629.

Hajnoczky, G., Csordas, G., Das, S., Garcia-Perez, C., Saotome, M., Sinha Roy, S. and Yi,
M., 2006. Mitochondrial calcium signalling and cell death: approaches for assessing
the role of mitochondrial Ca^{2+} uptake in apoptosis. Cell Calcium. 40, 553-560.

Harding, A. E. and Sweeney, M. G., 1994. Leber's hereditary optic neuropathy. In:
Schapira, A. H. V. and DiMauro, S. (Eds.), Mitochondrial Disorders in Neurology.
Butterworth-Heinemann, pp. 181-198.

Harding, A. E., Sweeney, M. G., Govan, G. G. and Riordan-Eva, P., 1995. Pedigree
analysis in Leber hereditary optic neuropathy families with a pathogenic mtDNA
mutation. Am J Hum Genet. 57, 77-86.

Head, E., Liu, J., Hagen, T. M., Muggenburg, B. A., Milgram, N. W., Ames, B. N. and
Cotman, C. W., 2002. Oxidative damage increases with age in a canine model of
human brain aging. J Neurochem. 82, 375-381.

Hoek, J. B., Walajtys-Rode, E. and Wang, X., 1997. Hormonal stimulation, mitochondrial
Ca^{2+} accumulation, and the control of the mitochondrial permeability transition in
intact hepatocytes. Mol Cell Biochem. 174, 173-179.

Holt, I. J., Miller, D. H. and Harding, A. E., 1989. Genetic heterogeneity and mitochondrial
DNA heteroplasmy in Leber's hereditary optic neuropathy. J Med Genet. 26, 739-
743.

Howell, N., 2003. LHON and other optic nerve atrophies: the mitochondrial connection.
Dev Ophthalmol. 37, 94-108.

Ichas, F. and Mazat, J. P., 1998. From calcium signaling to cell death: two conformations

for the mitochondrial permeability transition pore. Switching from low- to high-conductance state. Biochim Biophys Acta. 1366, 33-50.

Jacobson, J. and Duchen, M. R., 2004. Interplay between mitochondria and cellular calcium signalling. Mol Cell Biochem. 256-257, 209-218.

Jacquard, C., Trioulier, Y., Cosker, F., Escartin, C., Bizat, N., Hantraye, P., Cancela, J. M., Bonvento, G. and Brouillet, E., 2006. Brain mitochondrial defects amplify intracellular [Ca^{2+}] rise and neurodegeneration but not Ca^{2+} entry during NMDA receptor activation. Faseb J. 20, 1021-1023.

Jakubowski, W. and Bartosz, G., 2000. 2,7-dichlorofluorescin oxidation and reactive oxygen species: what does it measure? Cell Biol Int. 24, 757-760.

Johns, D. R., Heher, K. L., Miller, N. R. and Smith, K. H., 1993. Leber's hereditary optic neuropathy. Clinical manifestations of the 14484 mutation. Arch Ophthalmol. 111, 495-498.

Johns, D. R. and Colby, K. A., 2002. Treatment of Leber's hereditary optic neuropathy: theory to practice. Semin Ophthalmol. 17, 33-38.

Jordan, J., Fernandez-Gomez, F. J., Ramos, M., Ikuta, I., Aguirre, N. and Galindo, M. F., 2007. Minocycline and cytoprotection: shedding new light on a shadowy controversy. Curr Drug Deliv. 4, 225-231.

Kantrow, S. P. and Piantadosi, C. A., 1997. Release of cytochrome c from liver mitochondria during permeability transition. Biochem Biophys Res Commun. 232, 669-671.

Kasapoglu, M. and Ozben, T., 2001. Alterations of antioxidant enzymes and oxidative stress markers in aging. Exp Gerontol. 36, 209-220.

Keilhoff, G., Langnaese, K., Wolf, G. and Fansa, H., 2007. Inhibiting effect of minocycline on the regeneration of peripheral nerves. Dev Neurobiol. 67, 1382-1395.

Kerrison, J. B. and Newman, N. J., 1997. Clinical spectrum of Leber's hereditary optic neuropathy. Clin Neurosci. 4, 295-301.

Kim, R., Emi, M. and Tanabe, K., 2006. Role of mitochondria as the gardens of cell death. Cancer Chemother Pharmacol. 57, 545-553.

Kirichok, Y., Krapivinsky, G. and Clapham, D. E., 2004. The mitochondrial calcium uniporter is a highly selective ion channel. Nature. 427, 360-364.

Kitamura, Y., Miyamura, A., Takata, K., Inden, M., Tsuchiya, D., Nakamura, K. and Taniguchi, T., 2003. Possible involvement of both endoplasmic reticulum-and

mitochondria-dependent pathways in thapsigargin-induced apoptosis in human neuroblastoma SH-SY5Y cells. J Pharmacol Sci. 92, 228-236.

Kondo, K., 1996. Rising prevalence of neurodegenerative diseases worldwide. Intern Med. 35, 238.

Korge, P. and Weiss, J. N., 1999. Thapsigargin directly induces the mitochondrial permeability transition. Eur J Biochem. 265, 273-280.

Kraus, R. L., Pasieczny, R., Lariosa-Willingham, K., Turner, M. S., Jiang, A. and Trauger, J. W., 2005. Antioxidant properties of minocycline: neuroprotection in an oxidative stress assay and direct radical-scavenging activity. J Neurochem. 94, 819-827.

Lampl, Y., Boaz, M., Gilad, R., Lorberboym, M., Dabby, R., Rapoport, A., Anca-Hershkowitz, M. and Sadeh, M., 2007. Minocycline treatment in acute stroke: an open-label, evaluator-blinded study. Neurology. 69, 1404-1410.

Lee, S. M., Yune, T. Y., Kim, S. J., Kim, Y. C., Oh, Y. J., Markelonis, G. J. and Oh, T. H., 2004. Minocycline inhibits apoptotic cell death via attenuation of TNF-alpha expression following iNOS/NO induction by lipopolysaccharide in neuron/glia co-cultures. J Neurochem. 91, 568-578.

Leist, M., Single, B., Castoldi, A. F., Kuhnle, S. and Nicotera, P., 1997. Intracellular adenosine triphosphate (ATP) concentration: a switch in the decision between apoptosis and necrosis. J Exp Med. 185, 1481-1486.

Lin, M. T. and Beal, M. F., 2006. Mitochondrial dysfunction and oxidative stress in neurodegenerative diseases. Nature. 443, 787-795.

Lowry, O. H., Rosebrough, N. J., Farr, A. L. and Randall, R. J., 1951. Protein measurement with the Folin phenol reagent. J Biol Chem. 193, 265-275.

Lytton, J., Westlin, M. and Hanley, M. R., 1991. Thapsigargin inhibits the sarcoplasmic or endoplasmic reticulum Ca-ATPase family of calcium pumps. J Biol Chem. 266, 17067-17071.

Macmillan, C., Kirkham, T., Fu, K., Allison, V., Andermann, E., Chitayat, D., Fortier, D., Gans, M., Hare, H., Quercia, N., Zackon, D. and Shoubridge, E. A., 1998. Pedigree analysis of French Canadian families with T14484C Leber's hereditary optic neuropathy. Neurology. 50, 417-422.

Maher, P., 2005. The effects of stress and aging on glutathione metabolism. Ageing Res Rev. 4, 288-314.

Man, P. Y., Turnbull, D. M. and Chinnery, P. F., 2002. Leber hereditary optic neuropathy. J

Med Genet. 39, 162-169.

Man, P. Y., Griffiths, P. G., Brown, D. T., Howell, N., Turnbull, D. M. and Chinnery, P. F., 2003. The epidemiology of Leber hereditary optic neuropathy in the North East of England. Am J Hum Genet. 72, 333-339.

Mathai, J. P., Germain, M. and Shore, G. C., 2005. BH3-only BIK regulates BAX,BAK-dependent release of Ca^{2+} from endoplasmic reticulum stores and mitochondrial apoptosis during stress-induced cell death. J Biol Chem. 280, 23829-23836.

Mievis, S., Levivier, M., Communi, D., Vassart, G., Brotchi, J., Ledent, C. and Blum, D., 2007. Lack of Minocycline Efficiency in Genetic Models of Huntington's Disease. Neuromolecular Med. 9, 47-54.

Milane, A., Fernandez, C., Bensimon, G., Meininger, V., Farinotti, R., 2007. Simple Liquid Chromatographic Determination of Minocycline in Brain and Plasma. Chromatographia. 65, 277-281.

Mroczek-Tonska, K., Kisiel, B., Piechota, J. and Bartnik, E., 2003. Leber hereditary optic neuropathy--a disease with a known molecular basis but a mysterious mechanism of pathology. J Appl Genet. 44, 529-538.

NET-PD, T. N., 2006. A randomized, double-blind, futility clinical trial of creatine and minocycline in early Parkinson disease. Neurology. 66, 664-671.

Newman, N. J., Lott, M. T. and Wallace, D. C., 1991. The clinical characteristics of pedigrees of Leber's hereditary optic neuropathy with the 11778 mutation. Am J Ophthalmol. 111, 750-762.

Nicolli, A., Basso, E., Petronilli, V., Wenger, R. M. and Bernardi, P., 1996. Interactions of cyclophilin with the mitochondrial inner membrane and regulation of the permeability transition pore, and cyclosporin A-sensitive channel. J Biol Chem. 271, 2185-2192.

Nieminen, A. L., Petrie, T. G., Lemasters, J. J. and Selman, W. R., 1996. Cyclosporin A delays mitochondrial depolarization induced by N-methyl-D-aspartate in cortical neurons: evidence of the mitochondrial permeability transition. Neuroscience. 75, 993-997.

Novotny, E. J., Jr., Singh, G., Wallace, D. C., Dorfman, L. J., Louis, A., Sogg, R. L. and Steinman, L., 1986. Leber's disease and dystonia: a mitochondrial disease. Neurology. 36, 1053-1060.

O'Dell, J. R., Blakely, K. W., Mallek, J. A., Eckhoff, P. J., Leff, R. D., Wees, S. J., Sems, K.

M., Fernandez, A. M., Palmer, W. R., Klassen, L. W., Paulsen, G. A., Haire, C. E. and Moore, G. F., 2001. Treatment of early seropositive rheumatoid arthritis: a two-year, double-blind comparison of minocycline and hydroxychloroquine. Arthritis Rheum. 44, 2235-2241.

Petrozzi, L., Ricci, G., Giglioli, N. J., Siciliano, G. and Mancuso, M., 2007. Mitochondria and neurodegeneration. Biosci Rep. 27, 87-104.

Pi, R., Li, W., Lee, N. T., Chan, H. H., Pu, Y., Chan, L. N., Sucher, N. J., Chang, D. C., Li, M. and Han, Y., 2004. Minocycline prevents glutamate-induced apoptosis of cerebellar granule neurons by differential regulation of p38 and Akt pathways. J Neurochem. 91, 1219-1230.

Pontieri, F. E., Ricci, A., Pellicano, C., Benincasa, D. and Buttarelli, F. R., 2005. Minocycline in amyotrophic lateral sclerosis: a pilot study. Neurol Sci. 26, 285-287.

Puomila, A., Hamalainen, P., Kivioja, S., Savontaus, M. L., Koivumaki, S., Huoponen, K. and Nikoskelainen, E., 2007. Epidemiology and penetrance of Leber hereditary optic neuropathy in Finland. Eur J Hum Genet.

Qi, X., Sun, L., Hauswirth, W. W., Lewin, A. S. and Guy, J., 2007. Use of mitochondrial antioxidant defenses for rescue of cells with a Leber hereditary optic neuropathy-causing mutation. Arch Ophthalmol. 125, 268-272.

Qi, X., Sun, L., Lewin, A. S., Hauswirth, W. W. and Guy, J., 2007. The mutant human ND4 subunit of complex I induces optic neuropathy in the mouse. Invest Ophthalmol Vis Sci. 48, 1-10.

Rapizzi, E., Pinton, P., Szabadkai, G., Wieckowski, M. R., Vandecasteele, G., Baird, G., Tuft, R. A., Fogarty, K. E. and Rizzuto, R., 2002. Recombinant expression of the voltage-dependent anion channel enhances the transfer of Ca^{2+} microdomains to mitochondria. J Cell Biol. 159, 613-624.

Rauen, T., Rothstein, J. D. and Wassle, H., 1996. Differential expression of three glutamate transporter subtypes in the rat retina. Cell Tissue Res. 286, 325-336.

Rizzuto, R., Bernardi, P. and Pozzan, T., 2000. Mitochondria as all-round players of the calcium game. J Physiol. 529 Pt 1, 37-47.

Sadun, A. A., Carelli, V., Salomao, S. R., Berezovsky, A., Quiros, P., Sadun, F., DeNegri, A. M., Andrade, R., Schein, S. and Belfort, R., 2002. A very large Brazilian pedigree with 11778 Leber's hereditary optic neuropathy. Trans Am Ophthalmol Soc. 100, 169-178.

Sadun, A. A., Carelli, V., Salomao, S. R., Berezovsky, A., Quiros, P. A., Sadun, F., DeNegri, A. M., Andrade, R., Moraes, M., Passos, A., Kjaer, P., Pereira, J., Valentino, M. L., Schein, S. and Belfort, R., 2003. Extensive investigation of a large Brazilian pedigree of 11778/haplogroup J Leber hereditary optic neuropathy. Am J Ophthalmol. 136, 231-238.

Sadun, F., De Negri, A. M., Carelli, V., Salomao, S. R., Berezovsky, A., Andrade, R., Moraes, M., Passos, A., Belfort, R., da Rosa, A. B., Quiros, P. and Sadun, A. A., 2004. Ophthalmologic findings in a large pedigree of 11778/Haplogroup J Leber hereditary optic neuropathy. Am J Ophthalmol. 137, 271-277.

Sanchez Mejia, R. O., Ona, V. O., Li, M. and Friedlander, R. M., 2001. Minocycline reduces traumatic brain injury-mediated caspase-1 activation, tissue damage, and neurological dysfunction. Neurosurgery. 48, 1393-1399; discussion 1399-1401.

Scaduto, R. C., Jr. and Grotyohann, L. W., 1999. Measurement of mitochondrial membrane potential using fluorescent rhodamine derivatives. Biophys J. 76, 469-477.

Schinder, A. F., Olson, E. C., Spitzer, N. C. and Montal, M., 1996. Mitochondrial dysfunction is a primary event in glutamate neurotoxicity. J Neurosci. 16, 6125-6133.

Scorrano, L., Penzo, D., Petronilli, V., Pagano, F. and Bernardi, P., 2001. Arachidonic acid causes cell death through the mitochondrial permeability transition. Implications for tumor necrosis factor-alpha aopototic signaling. J Biol Chem. 276, 12035-12040.

Shoffner, J. M., Brown, M. D., Stugard, C., Jun, A. S., Pollock, S., Haas, R. H., Kaufman, A., Koontz, D., Kim, Y., Graham, J. R. and et al., 1995. Leber's hereditary optic neuropathy plus dystonia is caused by a mitochondrial DNA point mutation. Ann Neurol. 38, 163-169.

Singh, G., Lott, M. T. and Wallace, D. C., 1989. A mitochondrial DNA mutation as a cause of Leber's hereditary optic neuropathy. N Engl J Med. 320, 1300-1305.

Smaili, S. S., Hsu, Y. T., Youle, R. J. and Russell, J. T., 2000. Mitochondria in Ca^{2+} signaling and apoptosis. J Bioenerg Biomembr. 32, 35-46.

Smith, P. K., Krohn, R. I., Hermanson, G. T., Mallia, A. K., Gartner, F. H., Provenzano, M. D., Fujimoto, E. K., Goeke, N. M., Olson, B. J. and Klenk, D. C., 1985. Measurement of protein using bicinchoninic acid. Anal Biochem. 150, 76-85.

Starkov, A. A., Chinopoulos, C. and Fiskum, G., 2004. Mitochondrial calcium and oxidative stress as mediators of ischemic brain injury. Cell Calcium. 36, 257-264.

Stirling, D. P., Khodarahmi, K., Liu, J., McPhail, L. T., McBride, C. B., Steeves, J. D., Ramer, M. S., Tetzlaff, W., 2004. Minocycline treatment reduces delayed oligodendrocyte death, attenuates axonal dieback, and improves functional outcome after spinal cord injury. . J Neurosci. 3;24(9), 2182-2190.

Swerdlow, R. H., 2002. Mitochondrial DNA--related mitochondrial dysfunction in neurodegenerative diseases. Arch Pathol Lab Med. 126, 271-280.

Takeyama, N., Matsuo, N. and Tanaka, T., 1993. Oxidative damage to mitochondria is mediated by the Ca^{2+}-dependent inner-membrane permeability transition. Biochem J. 294 (Pt 3), 719-725.

Teplova, V., Evtodienko, Y., Odinokova, I., Kruglov, A. and Kudrjavtsev, A., 2000. Suppression of mitochondrial permeability transition pore and induction of lymphoma P388 cell death by cyclosporin A. IUBMB Life. 50, 75-80.

Tikka, T. M. and Koistinaho, J. E., 2001. Minocycline provides neuroprotection against N-methyl-D-aspartate neurotoxicity by inhibiting microglia. J Immunol. 166, 7527-7533.

Tomas-Camardiel, M., Rite, I., Herrera, A. J., de Pablos, R. M., Cano, J., Machado, A. and Venero, J. L., 2004. Minocycline reduces the lipopolysaccharide-induced inflammatory reaction, peroxynitrite-mediated nitration of proteins, disruption of the blood-brain barrier, and damage in the nigral dopaminergic system. Neurobiol Dis. 16, 190-201.

Tsao, K., Aitken, P. A. and Johns, D. R., 1999. Smoking as an aetiological factor in a pedigree with Leber's hereditary optic neuropathy. Br J Ophthalmol. 83, 577-581.

Tsujimoto, Y., Nakagawa, T. and Shimizu, S., 2006. Mitochondrial membrane permeability transition and cell death. Biochim Biophys Acta. 1757, 1297-1300.

van Loo, G., Schotte, P., van Gurp, M., Demol, H., Hoorelbeke, B., Gevaert, K., Rodriguez, I., Ruiz-Carrillo, A., Vandekerckhove, J., Declercq, W., Beyaert, R. and Vandenabeele, P., 2001. Endonuclease G: a mitochondrial protein released in apoptosis and involved in caspase-independent DNA degradation. Cell Death Differ. 8, 1136-1142.

Vercesi, A. E., Moreno, S. N., Bernardes, C. F., Meinicke, A. R., Fernandes, E. C. and Docampo, R., 1993. Thapsigargin causes Ca^{2+} release and collapse of the membrane potential of Trypanosoma brucei mitochondria in situ and of isolated rat liver mitochondria. J Biol Chem. 268, 8564-8568.

Vergun, O., Keelan, J., Khodorov, B. I. and Duchen, M. R., 1999. Glutamate-induced mitochondrial depolarisation and perturbation of calcium homeostasis in cultured rat hippocampal neurones. J Physiol. 519 Pt 2, 451-466.

Vina, J., Borras, C., Gambini, J., Sastre, J. and Pallardo, F. V., 2005. Why females live longer than males? Importance of the upregulation of longevity-associated genes by oestrogenic compounds. FEBS Lett. 579, 2541-2545.

Wallace, D. C., Singh, G., Lott, M. T., Hodge, J. A., Schurr, T. G., Lezza, A. M., Elsas, L. J., 2nd and Nikoskelainen, E. K., 1988. Mitochondrial DNA mutation associated with Leber's hereditary optic neuropathy. Science. 242, 1427-1430.

Wang, X., Zhu, S., Drozda, M., Zhang, W., Stavrovskaya, I. G., Cattaneo, E., Ferrante, R. J., Kristal, B. S. and Friedlander, R. M., 2003. Minocycline inhibits caspase-independent and -dependent mitochondrial cell death pathways in models of Huntington's disease. Proc Natl Acad Sci U S A. 100, 10483-10487.

Wang, J., Wei, Q., Wang, C. Y., Hill, W. D., Hess, D. C. and Dong, Z., 2004. Minocycline up-regulates Bcl-2 and protects against cell death in mitochondria. J Biol Chem. 279, 19948-19954.

Wei, Y. H. and Lee, H. C., 2002. Oxidative stress, mitochondrial DNA mutation, and impairment of antioxidant enzymes in aging. Exp Biol Med (Maywood). 227, 671-682.

Wei, X., Zhao, L., Liu, J., Dodel, R. C., Farlow, M. R. and Du, Y., 2005. Minocycline prevents gentamicin-induced ototoxicity by inhibiting p38 MAP kinase phosphorylation and caspase 3 activation. Neuroscience. 131, 513-521.

Weissman, L., de Souza-Pinto, N. C., Stevnsner, T. and Bohr, V. A., 2007. DNA repair, mitochondria, and neurodegeneration. Neuroscience. 145, 1318-1329.

Whiteman, M. and Halliwell, B., 1997. Prevention of peroxynitrite-dependent tyrosine nitration and inactivation of alpha1-antiproteinase by antibiotics. Free Radic Res. 26, 49-56.

Wiesner, R. J., Ruegg, J. C. and Morano, I., 1992. Counting target molecules by exponential polymerase chain reaction: copy number of mitochondrial DNA in rat tissues. Biochem Biophys Res Commun. 183, 553-559.

Wiesner, R. J., Zsurka, G. and Kunz, W. S., 2006. Mitochondrial DNA damage and the aging process: facts and imaginations. Free Radic Res. 40, 1284-1294.

Wong, A., Cavelier, L., Collins-Schramm, H. E., Seldin, M. F., McGrogan, M., Savontaus,

M. L. and Cortopassi, G. A., 2002. Differentiation-specific effects of LHON mutations introduced into neuronal NT2 cells. Hum Mol Genet. 11, 431-438.

Woodfield, K., Ruck, A., Brdiczka, D. and Halestrap, A. P., 1998. Direct demonstration of a specific interaction between cyclophilin-D and the adenine nucleotide translocase confirms their role in the mitochondrial permeability transition. Biochem J. 336 (Pt 2), 287-290.

Wu, D. C., Jackson-Lewis, V., Vila, M., Tieu, K., Teismann, P., Vadseth, C., Choi, D. K., Ischiropoulos, H. and Przedborski, S., 2002. Blockade of microglial activation is neuroprotective in the 1-methyl-4-phenyl-1,2,3,6-tetrahydropyridine mouse model of Parkinson disease. J Neurosci. 22, 1763-1771.

Yamazaki, T., Muramoto, M., Oe, T., Morikawa, N., Okitsu, O., Nagashima, T., Nishimura, S., Katayama, Y. and Kita, Y., 2006. Diclofenac, a non-steroidal anti-inflammatory drug, suppresses apoptosis induced by endoplasmic reticulum stresses by inhibiting caspase signaling. Neuropharmacology. 50, 558-567.

Yong, V. W., Wells, J., Giuliani, F., Casha, S., Power, C. and Metz, L. M., 2004. The promise of minocycline in neurology. Lancet Neurol. 3, 744-751.

Yoshida, I., Monji, A., Tashiro, K., Nakamura, K., Inoue, R. and Kanba, S., 2006. Depletion of intracellular Ca^{2+} store itself may be a major factor in thapsigargin-induced ER stress and apoptosis in PC12 cells. Neurochem Int. 48, 696-702.

Yrjanheikki, J., Keinanen, R., Pellikka, M., Hokfelt, T. and Koistinaho, J., 1998. Tetracyclines inhibit microglial activation and are neuroprotective in global brain ischemia. Proc Natl Acad Sci U S A. 95, 15769-15774.

Yrjanheikki, J., Tikka, T., Keinanen, R., Goldsteins, G., Chan, P. H. and Koistinaho, J., 1999. A tetracycline derivative, minocycline, reduces inflammation and protects against focal cerebral ischemia with a wide therapeutic window. Proc Natl Acad Sci U S A. 96, 13496-13500.

Yune, T. Y., Lee, J. Y., Jung, G. Y., Kim, S. J., Jiang, M. H., Kim, Y. C., Oh, Y. J., Markelonis, G. J. and Oh, T. H., 2007. Minocycline alleviates death of oligodendrocytes by inhibiting pro-nerve growth factor production in microglia after spinal cord injury. J Neurosci. 27, 7751-7761.

Zamzami, N., Marchetti, P., Castedo, M., Hirsch, T., Susin, S. A., Masse, B. and Kroemer, G., 1996. Inhibitors of permeability transition interfere with the disruption of the mitochondrial transmembrane potential during apoptosis. FEBS Lett. 384, 53-57.

Zanna, C., Ghelli, A., Porcelli, A. M., Carelli, V., Martinuzzi, A. and Rugolo, M., 2003. Apoptotic cell death of cybrid cells bearing Leber's hereditary optic neuropathy mutations is caspase independent. Ann N Y Acad Sci. 1010, 213-217.

Zanna, C., Ghelli, A., Porcelli, A. M., Martinuzzi, A., Carelli, V. and Rugolo, M., 2005. Caspase-independent death of Leber's hereditary optic neuropathy cybrids is driven by energetic failure and mediated by AIF and Endonuclease G. Apoptosis. 10, 997-1007.

Zhu, S., Stavrovskaya, I. G., Drozda, M., Kim, B. Y., Ona, V., Li, M., Sarang, S., Liu, A. S., Hartley, D. M., Wu du, C., Gullans, S., Ferrante, R. J., Przedborski, S., Kristal, B. S. and Friedlander, R. M., 2002. Minocycline inhibits cytochrome c release and delays progression of amyotrophic lateral sclerosis in mice. Nature. 417, 74-78.

Zoratti, M. and Szabo, I., 1995. The mitochondrial permeability transition. Biochim Biophys Acta. 1241, 139-176.

CURRICULUM VITAE

Personal details:

Name:	Mohammad Fahad Haroon
Date of birth:	13/11/1976
Nationality:	Indian
Private address:	Fermersleber Weg 45c
	39112 Magdeburg
Working address:	Leipziger Str. 44
	39120 Magdeburg
Telephone:	+49-3916714367
Fax:	+49-3916714365
E-mail:	Fahad.Haroon@med.ovgu.de

Educational Qualifications:

September 2004 – December 2007: PhD student / University of Magdeburg

Enrolled as PhD student at Institute of Medical Neurobiology, Otto-von-Guericke University, Magdeburg, Germany

PhD research Project:

"Pathogenetic mechanisms of mitochondrial mediated Neurodegeneration and Protection strategies" (funded by NBL3-Partnerfocusgruppe)

2003 - August 2004: Research student in Pharmacy / Hamdard University, New Delhi

Worked in the Department of Pharmacology, Hamdard University, Delhi

Project supervised by Prof K.K.Pillai and Dr S.E. Haq:

"Investigation of the effects of cromolyn sodium on fentanyl induced cardioprotection in doxorubicin induced myocardial infarction"

2000-2002: Post Graduation in Pharmacy / Hamdard University, New Delhi

Student at Faculty of Pharmacy in the Department of Pharmacology

M. Pharm. Thesis Project:

"Influence of fentanyl in myocardial infarction and global ischemia and its modulation by cromolyn sodium in rat hearts in: (i) isoproterenol induced myocardial infarction and (ii) Langendroff's isolated heart"

1996 - 2000: Graduation in Pharmacy / Hamdard University, New Delhi

1993 - 1995: Secondary school / Indian Embassy School, Jeddah, Saudia Arabia

Research Experience:

January 2008 – Till date (December 2008):
Working in the Institute of Medical Microbiology, Otto von Guericke University, Magdeburg, Germany as a postdoctoral fellow.

September 2004 – December 2007:
Worked in the Institute of Medical Neurobiology, Otto von Guericke University, Magdeburg, Germany and acquired knowledge of basic cell culturing techniques, confocal microscopy, molecular biological techniques and staining procedures. The basis of research was the mitochondriopathy linked to LHON disease and devising of pharmacological protective strategies.

2003-August 2004:
Worked in the Department of Pharmacology, Hamdard University, Delhi under supervision of Prof. K.K.Pillai and Dr. S.E. Haq. We had investigated the effect cromolyn sodium on fentanyl induced cardioprotection in doxorubicin induced myocardial infarction.

2000-2002:
During my first year of Masters of Pharmacy, I was familiarized with various experimental aspect of basic pharmacology (Bioassays of endogenous compounds, estimation of pA2 value, open field test, forced swimming test, spontaneous locomotion, elevated plus maze, Rotarod, active and passive avoidance, various models of epilepsy and pain among several other procedures employed for screening of drugs effecting central nervous system). Master of Pharmacy thesis project was completed under supervision of Prof. K.K.Pillai.

Awards and Scholarships:

Qualified Graduate Aptitude Test for Engineers 2000 with 98 percentile and awarded a junior research fellowship by UGC Govt. of India, from August 2000 - January 2002.

Technical Expertise:

1. Confocal Microscopy (Pascal) and Fluorescence Microscopy (Axiophot); Live cell calcium imaging
2. Techniques for immunocytochemistry for detecting different endogenous marker using immuno-fluorescence.
3. Primary (Cortical), organotypic and permanent Cell culturing techniques
4. Basic molecular biology techniques. Western blotting, RT-PCR, Tissue preparation and cryosectioning.
5. Biochemical Pharmacology: Estimation of various plasma and serum markers
6. Flame Photometer for mineral element detection and quantification
7. Basic research *in vivo* pharmacological screening techniques for evaluating anti-diabetic, antihyperlipidaemic, anti-inflammatory, anti-ulcer, cardiovascular and neuropsychiatric drugs
8. Statistical methods and operation of Graphpad Prism software

Publications:

- **Haroon M F**, Fatima A, Schoeler S, Gieseler A, Horn T F W, Kirches E, Wolf G and Kreutzmann P. Minocycline, a possible neuroprotective agent in Leber's hereditary optic neuropathy (LHON): studies of cybrid cells bearing 11778 mutation. **Neurobiology of Disease; Vol 28, Issue 3; December 2007; Pages 237-250.**

- Schoeler S, Winkler-Stuck K, Szibor R**, Haroon M F**, Gellerich F N, Chamaon K, Mawrin C, Kirches E. Glutathione depletion in antioxidant defense of differentiated NT2-LHON cybrids**. Neurobiology of Disease; Vol 25; Issue 3; March 2007; Pages 536-544.**

- Schoeler S, Hertel S, **Haroon M F,** Winkler-Stuck K, Mawrin C and Kirches E. Absence of major accumulation of mitochondrial ND5 mutations in Parkinson patient muscle. **Clinical Neuropathology; Vol 26; No 4; 2007; Pages 164-168.**

- Fatima A, **Haroon M F**, Wolf G, Engelmann M and Spina M G. Reduced urocortin 1 immunoreactivity in the non-preganglionic Edinger-Westphal nucleus during late pregnancy in rats. **Regulatory Peptides; Vol 143; 2007;Pages 34–38**

- Schild L, Makarow P, **Haroon F**, Krautwald K, Keilhoff G. Distinct H2O2 concentration promotes proliferation of tumour cells after transient oxygen/glucose deprivation. **Free Radical Research; 2008 Mar; Vol 42(3): Pages 237-43.**

- Gieseler A, Schultze A T, Kupsch K, **Haroon M F**, Wolf G, Siemen D, Kreutzmann P. Inhibitory modulation of the mitochondrial permeability transition by minocycline. **Biochem Pharmacol. 2008 Nov.** doi:10.1016/j.bcp.2008.11.003

Conference attended:

- Presented a lecture titled "Minocycline in LHON cybrid cells alleviates calcium deregulation. The role of mitochondrial permeability transition pore" at **The 5th Annual Conference of Society for Free Radicals Research – India Jan. 16-18 2006.**

- **Haroon M F**, Horn T F W, Kirches E and Wolf G. Minocycline in LHON cybrid cells alleviates calcium deregulation. The role of mitochondrial permeability transition pore. **Poster presented at the 4th International Symposium on Neuroprotection and Neurorepair Cerebral Ischemia and Stroke, May 3-6, 2006 in Magdeburg, Germany.**

- **Haroon M F**, Kreutzmann P, Kirches E and Wolf G. Oxidative stress in LHON (Leber's hereditary optic neuropathy) cybrid cell model: a study of the antioxidant effect of minocycline. **Poster presented at "2nd Joint French-German NO-Meeting", Hamburg, Germany, October 5 - 7, 2006**

- **Haroon M F**, Kirches E, Wolf G and Kreutzmann P. Nuclear translocation of AIF involved in cell death induced by thapsigargin in a LHON cybrid cell model. **Poster presented at the 5th Federal European Neuroscience Scociety Forum, Geneva, Switzerland July 12 – 16, 2008**